MZ-TH/95-19
FTUV/95-52
IFIC/95-54
January 1996

Polar Angle Dependence of the Alignment Polarization of Quarks Produced in e^+e^--Annihilation

S. Groote*, J.G. Körner*

Institut für Physik, Johannes Gutenberg-Universität
Staudingerweg 7, D-55099 Mainz, Germany.

M.M. Tung**

Departament de Física Teòrica, Universitat de València
and IFIC, Centre Mixte Universitat València — CSIC,
C/ Dr. Moliner, 50, E-46100 Burjassot (València), Spain.

ABSTRACT

We calculate one-loop radiative QCD corrections to the three polarized and unpolarized structure functions that determine the beam-quark polar angle dependence of the alignment (or longitudinal) polarization of light and heavy quarks produced in e^+e^--annihilations. We present analytical and numerical results for the alignment polarization and its polar angle dependence. We discuss in some detail the zero-mass limit of our results and the role of the anomalous spin-flip contributions to the polarization observables in the zero-mass limit. Our discussion includes transverse and longitudinal beam polarization effects.

*Supported in part by the BMFT, FRG, under contract 06MZ566,
and by HUCAM, EU, under contract CHRX-CT94-0579

**Feodor-Lynen Fellow

1 Introduction

This is the fifth and final paper in a series of papers devoted to the $O(\alpha_s)$ determination of the polarization of quarks produced in e^+e^--annihilations. In the first paper of this series [1] we calculated the mean alignment polarization (sometimes also called longitudinal or helicity polarization) of the quark. i.e. the alignment polarization averaged w.r.t. the relative beam-event orientation. One of us derived convenient Schwinger-type representations for the structure functions appearing in the polarization expressions in [2]. In a third paper we determined the longitudinal component of the quark's alignment polarization, which vanishes at the Born term level [3]. The fourth paper [4] gave results on the two transverse components of the quark's polarization (perpendicular and normal, also sometimes referred to as in-the-plane and out-of-the-plane polarization). In the present final piece of work we present our results on the full polar angle dependence of the quark's alignment polarization w.r.t. the electron beam direction including beam polarization effects.

The full determination of the alignment polarization of the quark involves the calculation of three polarized and three unpolarized structure functions which are conveniently chosen as the helicity structure functions $H^\ell_{U,L,F}$ and $H_{U,L,F}$, respectively. The subscripts U, L and F label the relevant density matrix elements of the exchanged vector boson (γ_V,Z), where the polar angle dependence of the contributions of the three structure functions is given by $(1+\cos^2\theta)$ for U, $\sin^2\theta$ for L and $\cos\theta$ for F. We mention that some of the unpolarized helicity structure functions have been calculated before, i.e. the vector/vector (VV) contribution to H_U and H_L [5]† and the vector/axial-vector (VA) contribution to H_F [7]. We have verified the results of [5] and [7] and present new results on the axial-vector/axial-vector (AA) contribution to H_U and H_L in this paper, where the AA-contribution to $H_{U+L} = H_U + H_L$ was already written down in [1,2]. As concerns the polarized structure functions our results on H^ℓ_{U+L} and H^ℓ_L where given in [1,2,3]. This paper includes new results on the polarized structure functions H^ℓ_U and H^ℓ_F that are necessary to determine the full $\cos\theta$-dependence of the quark's alignment polarization.

†The VV-contribution to $H_{U+L} = H_U + H_L$ has been given a long time ago in the context of QED (see e.g. [6])

The paper is structured such that we start in Sec. 2 by listing the four independent tree-graph components of the hadron tensor (VV, AA, VA and AV) including its polarization dependence. The relevant helicity components of the structure functions $H_{U,L,F}$ and $H^{\ell}_{U,L,F}$ are obtained by covariant projections. We then proceed to integrate the projected tree-graph contributions over the full three-body phase-space and give analytical results for the once- and twice-integrated tree-graph cross sections. As is well familiar by now, the final expressions contain infrared (IR) divergences which we choose to regularize by introducing a small gluon mass. The tree-graph IR divergencies are cancelled by the corresponding IR divergencies of the one-loop contributions. Thus by adding in the loop contributions we finally arrive at finite results relevant for the total inclusive cross section integrated over the hard and the soft regions of the energy of the gluon as presented later on. In Sec. 2 we also detail the dependence of the polarization on the electroweak parameters including a discussion of beam polarization effects.

In Sec. 3 we first focus on the soft-gluon region and give results on the polar angle dependence of the alignment polarization of the quark with their typical logarithmic dependence on the gluon-energy cut. The hard-gluon contribution is given by the complement of the soft-gluon contribution, i.e. as the difference of the full $O(\alpha_s)$ and the soft-gluon contribution. Since we provide numerically stable expressions for the latter two contributions, the hard-gluon contribution can be evaluated in a numerically stable way. In Sec. 4 we consider the zero quark mass case and calculate the three relevant polarized and unpolarized structure functions using helicity methods and dimensional reduction as regularization method. In this way one can keep out of the way of the notorious γ_5-problem when calculating e.g. the VA-contribution to the F-type unpolarized structure function. We compare the mass-zero results with the mass-zero limit of the corresponding structure function expressions in Sec. 3 and identify the global anomalous spin-flip contributions to the QCD($m \to 0$) polarized structure functions. Finally, Sec. 5 contains our summary and our conclusions. In Appendix A we catalogue some integrals that appear in the tree-graph integrations in Sec. 2, in Appendix B we list some standard $O(\alpha_s)$ rate functions needed for the rate expressions in Sec. 3. In Appendix C, finally, we consider the case of polarized and unpolarized quark production from transversely and longitudinally polarized e^+e^--beams.

2 $O(\alpha_s)$ tree-graph contributions and total rates

For the three body process $(\gamma_V, Z) \to q(p_1)+\overline{q}(p_2)+g(p_3)$ (see Fig. 1) we define a polarized hadron tensor according to ($q = p_1 + p_2 + p_3$)

$$H_{\mu\nu}(q, p_1, p_2, s) = \sum_{\overline{q},g \text{ spins}} \langle q\,\overline{q}\,g|j_\mu|0\rangle\langle 0|j_\nu^\dagger|q\,\overline{q}\,g\rangle. \tag{1}$$

The hadron tensor depends on the vector (V) and axial-vector (A) composition of the currents in Eq. (1). One has altogether four independent components $H^i_{\mu\nu}$ ($i = 1, 2, 3, 4$) which are defined according to (V: γ_μ, A: $\gamma_\mu\gamma_5$)

$$\begin{aligned} H^1_{\mu\nu} &= \frac{1}{2}(H^{VV}_{\mu\nu} + H^{AA}_{\mu\nu}) \qquad H^2_{\mu\nu} = \frac{1}{2}(H^{VV}_{\mu\nu} - H^{AA}_{\mu\nu}) \\ H^3_{\mu\nu} &= \frac{i}{2}(H^{VA}_{\mu\nu} - H^{AV}_{\mu\nu}) \qquad H^4_{\mu\nu} = \frac{1}{2}(H^{VA}_{\mu\nu} + H^{AV}_{\mu\nu}). \end{aligned} \tag{2}$$

For the tree-graph contribution one calculates

$$\begin{aligned} H^1_{\mu\nu} &= \frac{g_s^2 N_C C_F}{2y^2z^2q^2}\Big[\, q^2(-(2-\xi)(\xi(y+z)^2 - 4yz(1-y-z)) + 4yz(y^2+z^2))g_{\mu\nu} \\ &\quad +16y^2z p_{1\mu}p_{1\nu} + 4(\xi y^2 - 4yz + 2\xi yz + 2y^2z + \xi z^2 + 2yz^2)(p_{1\mu}p_{2\nu} + p_{2\mu}p_{1\nu}) \\ &\quad +16yz^2 p_{2\mu}p_{2\nu} + 4z(-2y + \xi y + 2y^2 + \xi z)(p_{1\mu}p_{3\nu} + p_{3\mu}p_{1\nu}) \\ &\quad +4y(\xi y - 2z + \xi z + 2z^2)(p_{2\mu}p_{3\nu} + p_{3\mu}p_{2\nu})\,\Big] \\ &\quad +\frac{2img_s^2 N_C C_F}{y^2z^2q^4}\Big[\, q^2(2-\xi)y^2\varepsilon(\mu\nu p_1 s) - q^2(4yz - 2\xi yz + 2y^2z - 2yz^2)\varepsilon(\mu\nu p_2 s) \\ &\quad +q^2(2y^2 - \xi y^2 - 2yz + 2\xi yz + \xi z^2)\varepsilon(\mu\nu p_3 s) \\ &\quad -4y^2(p_{1\mu} + p_{3\mu})\varepsilon(\nu p_1 p_2 s) + 4y^2(p_{1\nu} + p_{3\nu})\varepsilon(\mu p_1 p_2 s) \\ &\quad +4y(yp_{1\mu} + zp_{2\mu} + yp_{3\mu})\varepsilon(\nu p_2 p_3 s) - 4y(yp_{1\nu} + zp_{2\nu} + yp_{3\nu})\varepsilon(\mu p_2 p_3 s)\,\Big] \end{aligned} \tag{3}$$

$$\begin{aligned} H^2_{\mu\nu} &= \frac{2m^2 g_s^2 N_C C_F}{y^2z^2q^4}\Big[\, -q^2(\xi(y+z)^2 - 4yz(1-y-z))g_{\mu\nu} + 8yzp_{3\mu}p_{3\nu}\,\Big] \\ &\quad +\frac{2img_s^2 N_C C_F}{y^2z^2q^4}\Big[\, q^2(\xi y^2 - 2yz + \xi yz + \xi z^2 + 4yz^2)\varepsilon(\mu\nu p_1 s) \\ &\quad -q^2\xi z(y-z)\varepsilon(\mu\nu p_2 s) + q^2\xi y(y-z)\varepsilon(\mu\nu p_3 s) \\ &\quad -4yz(p_{1\mu} + p_{3\mu})\varepsilon(\nu p_1 p_2 s) + 4yz(p_{1\nu} + p_{3\nu})\varepsilon(\mu p_1 p_2 s) \\ &\quad -4yz(p_{1\mu} - p_{2\mu} + p_{3\mu})\varepsilon(\nu p_1 p_3 s) + 4yz(p_{1\nu} - p_{2\nu} + p_{3\nu})\varepsilon(\mu p_1 p_3 s)\,\Big] \end{aligned} \tag{4}$$

$$
\begin{aligned}
H^3_{\mu\nu} &= \frac{2img_s^2N_CC_F}{y^2z^2q^4}\Big[-4yz(p_3s)(p_{1\mu}p_{2\nu}-p_{2\mu}p_{1\nu})+4yz(p_2s+p_3s)(p_{1\mu}p_{3\nu}-p_{3\mu}p_{1\nu})\\
&\quad -q^2(\xi y^2-4yz+2\xi yz+2y^2z+\xi z^2+4yz^2)(p_{1\mu}s_\nu-s_\mu p_{1\nu})\\
&\quad -2q^2yz^2(p_{2\mu}s_\nu-s_\mu p_{2\nu})-q^2(\xi y^2-2yz+\xi yz+2y^2z)(p_{3\mu}s_\nu-s_\mu p_{3\nu})\Big] \qquad (5)
\end{aligned}
$$

and

$$
\begin{aligned}
H^4_{\mu\nu} &= \frac{2ig_s^2N_CC_F}{y^2z^2q^4}\Big[-q^2(\xi y^2-4yz+2\xi yz-2y^2z+\xi z^2+2yz^2)\varepsilon(\mu\nu p_1p_2)\\
&\quad -q^2(2y^2-\xi y^2-2yz+2\xi yz+\xi z^2)\varepsilon(\mu\nu p_1p_3)+4q^2\xi y^2\varepsilon(\mu\nu p_2p_3)\\
&\quad +8y(yp_{1\mu}+zp_{2\mu}+yp_{3\mu})\varepsilon(\nu p_1p_2p_3)-8y(yp_{1\nu}+zp_{2\nu}+yp_{3\nu})\varepsilon(\mu p_1p_2p_3)\Big]\\
&\quad +\frac{2mg_s^2N_CC_F}{y^2z^2q^4}\Big[-q^2((\xi y^2-4yz+2\xi yz+2y^2z+\xi z^2+2yz^2)(p_2s)\\
&\qquad +(-2y^2+\xi y^2-2yz+2\xi yz+4y^2z+\xi z^2)(p_3s))g_{\mu\nu}\\
&\quad -4y^2(p_3s)(p_{1\mu}p_{2\nu}+p_{2\mu}p_{1\nu})+8yz(p_3s)p_{2\mu}p_{2\nu}\\
&\quad -4y(z(p_2s)+y(p_3s))(p_{2\mu}p_{3\nu}+p_{3\mu}p_{2\nu})+2q^2y^2z(p_{1\mu}s_\nu+s_\mu p_{1\nu})\\
&\quad +q^2(\xi y^2-4yz+2\xi yz+4y^2z+\xi z^2+2yz^2)(p_{2\mu}s_\nu+s_\mu p_{2\nu})\\
&\quad +q^2(-2yz+\xi yz+2y^2z+\xi z^2)(p_{3\mu}s_\nu+s_\mu p_{3\nu})\Big], \qquad (6)
\end{aligned}
$$

where we have accounted for the spin dependence of the hadron tensor by using the quark's spin projector $u(p_1,s)\bar{u}(p_1,s)=(\not{p}_1+m)\frac{1}{2}(1+\gamma_5\not{s})$ when calculating the trace according to Eq. (1). We have used the energy variables $y=1-2p_1\cdot q/q^2$ and $z=1-2p_2\cdot q/q^2$ and the abbreviation $\xi=4m^2/q^2$. Note that for the spin dependent contributions, $H^{1,2,3}_{\mu\nu}(s)$ are antisymmetric in μ and ν, while $H^4_{\mu\nu}(s)$ is symmetric in μ and ν. For the spin independent pieces, the nonvanishing contributions $H^{1,2}_{\mu\nu}$ are symmetric, $H^4_{\mu\nu}$ is antisymmetric in μ and ν, and there is no spin independent contribution to $H^3_{\mu\nu}$.

In this paper we are only concerned with the alignment polarization. The covariant form of the polarization four-vector associated with the alignment polarization is given by $s^{\ell\mu}=\xi^{-1/2}(\sqrt{(1-y)^2-\xi},0,0,1-y)$ ($s^\ell_\mu s^{\ell\mu}=-1$) which reduces to $s^{\ell\mu}=(0,0,0,1)$ in the rest system of the quark when $y=1-\sqrt{\xi}$. We then define unpolarized and polarized

structure functions $H^i_{\mu\nu}$ and $H^{i\ell}_{\mu\nu}$ $(i = 1, 2, 3, 4)$ according to

$$H^i_{\mu\nu} = H^i_{\mu\nu}(s^\ell) + H^i_{\mu\nu}(-s^\ell), \tag{7}$$

$$H^{i\ell}_{\mu\nu} = H^i_{\mu\nu}(s^\ell) - H^i_{\mu\nu}(-s^\ell). \tag{8}$$

In order to determine the polar angle dependence of the polarized and unpolarized cross section one turns to the helicity structure functions $H_U = H_{++} + H_{--}$, $H_L = H_{00}$ and $H_F = H_{++} - H_{--}$ which can be obtained from the covariant structure functions in Eqs. (7) and (8) by the appropiate helicity projections of the gauge boson,

$$H_{\lambda_{Z,\gamma}\lambda_{Z,\gamma}} = \varepsilon^\mu(\lambda_{Z,\gamma}) H_{\mu\nu} \varepsilon^{\nu *}(\lambda_{Z,\gamma}) \tag{9}$$

and the same for $H^\ell_{\mu\nu}$.

A convenient way of obtaining the helicity structure functions H_α $(\alpha = U, L, F)$ is by covariant projection,

$$H_U = \left(-\hat{g}^{\mu\nu} - \frac{\hat{p}_1^\mu \hat{p}_1^\nu}{p_{1z}^2}\right) H_{\mu\nu} \qquad H_L = \frac{\hat{p}_1^\mu \hat{p}_1^\nu}{p_{1z}^2} H_{\mu\nu} \qquad H_F = i\varepsilon^{\mu\nu\alpha\beta} \frac{\hat{p}_{1\alpha} q_\beta}{p_{1z}\sqrt{q^2}} H_{\mu\nu}, \tag{10}$$

where $\hat{g}_{\mu\nu} = g_{\mu\nu} - q_\mu q_\nu/q^2$ and $\hat{p}_{1\mu} = p_{1\mu} - (p_1 \cdot q) q_\mu/q^2$ are the four-transverse metric tensor and the four-transverse quark momentum, respectively. Note that the covariant projectors defined in Eq. (10) are (y, z)-independent and can thus be freely commuted with the y- and z-integrations to be done later on.

After all these preliminaries let us write down the differential polarized and unpolarized three-body e^+e^--cross sections, differential in $\cos\theta$ and in the two energy variables y and z. One has

$$\begin{aligned} \frac{d\sigma^\ell}{d\cos\theta\, dy\, dz} &= \frac{3}{8}(1 + \cos^2\theta) g_{14} \frac{d\sigma_U^{4\ell}}{dy\, dz} + \frac{3}{4}\sin^2\theta\ g_{14} \frac{d\sigma_L^{4\ell}}{dy\, dz} \\ &\quad + \frac{3}{4}\cos\theta \left(g_{41} \frac{d\sigma_F^{1\ell}}{dy\, dz} + g_{42} \frac{d\sigma_F^{2\ell}}{dy\, dz}\right) \qquad \text{and} \end{aligned} \tag{11}$$

$$\begin{aligned} \frac{d\sigma}{d\cos\theta\, dy\, dz} &= \frac{3}{8}(1 + \cos^2\theta) \left(g_{11} \frac{d\sigma_U^1}{dy\, dz} + g_{12} \frac{d\sigma_U^2}{dy\, dz}\right) \\ &\quad + \frac{3}{4}\sin^2\theta \left(g_{11} \frac{d\sigma_L^1}{dy\, dz} + g_{12} \frac{d\sigma_L^2}{dy\, dz}\right) + \frac{3}{4}\cos\theta\ g_{44} \frac{d\sigma_F^4}{dy\, dz} \end{aligned} \tag{12}$$

where, in terms of the helicity structure functions defined above, one has

$$\frac{d\sigma_\alpha^i}{dy\, dz} = \frac{\pi\alpha^2 v}{3q^4} \left\{\frac{q^2}{16\pi^2 v} H_\alpha^i\right\}. \tag{13}$$

($\alpha = U, L, F$) and the same for $\sigma^i_\alpha \to \sigma^{i\ell}_\alpha$ etc. The g_{ij} coupling factors appearing in Eqs. (11) and (12) specify the electroweak structure of the lepton-hadron interaction and are listed in Appendix C. The y, z and $\cos\theta$-dependent polarization $P^\ell(\cos\theta, y, z)$ is then given by the ratio of the polarized and unpolarized cross sections in Eqs. (11) and (12).

The generalization of the above cross section expressions to the case where one starts with "longitudinally" polarized beams is straightforward and amounts to the replacement (see Appendix C)

polarized:

$$\begin{aligned} g_{14} &\to [(1-h^-h^+)g_{14} + (h^- - h^+)g_{44}] \\ g_{4i} &\to [(h^- - h^+)g_{1i} + (1-h^-h^+)g_{4i}] \quad (i=1,2) \end{aligned} \tag{14}$$

unpolarized:

$$\begin{aligned} g_{1i} &\to [(1-h^-h^+)g_{1i} + (h^- - h^+)g_{4i}] \quad (i=1,2) \\ g_{44} &\to [(h^- - h^+)g_{14} + (1-h^-h^+)g_{44}] \end{aligned} \tag{15}$$

where h^- and h^+ ($-1 \le h^\pm \le +1$) denote the helicity polarization of the electron and the positron beam. Clearly there is no interaction between the beams when $h^+ = h^- = \pm 1$.

We have presented the results of calculating the full ($U + L$) and the longitudinal piece (L) of the polarized hadron tensor in [1,3]. Here we add the last building block, namely the polarized hadron tensor projected on its forward/backward component (F), where the requisite covariant projector has been given in Eq. (10). A straightforward calculation of the $O(\alpha_s)$ tree-graph contributions leads to

$$\begin{aligned} H_F^{1\ell}(y,z) &= \frac{8\pi\alpha_s N_C C_F}{(1-y)^2-\xi}\Bigg[\, 8 - 4\xi - \xi^2 - 2(2-\xi)(2-3\xi)\frac{1}{y} \\ &\quad -\xi(1-\xi)(2-\xi)\left(\frac{1}{y^2}+\frac{1}{z^2}\right) - 2\xi y - 4yz - 6\xi z - 4(2-\xi)(3-2\xi)\frac{1}{z} \\ &\quad +2(1-\xi)(2-\xi)^2\frac{1}{yz} + (4-2\xi-\xi^2)\frac{z}{y} + (28-14\xi+\xi^2)\frac{y}{z} \\ &\quad +2\xi(2-\xi)\frac{y}{z^2} - \xi(4-\xi)\frac{y^2}{z^2} + 4\frac{y^3}{z} + 2\xi\frac{y^3}{z^2} - 2(8-3\xi)\frac{y^2}{z}\Bigg] \end{aligned} \tag{16}$$

$$\begin{aligned} H_F^{2\ell}(y,z) &= \frac{8\pi\alpha_s N_C C_F}{(1-y)^2-\xi}\,\xi\Bigg[\, 4 + \xi - 2(2-3\xi)\frac{1}{y} - \xi(1-\xi)\left(\frac{1}{y^2}+\frac{1}{z^2}\right) \\ &\quad +4z - 4(3-2\xi)\frac{1}{z} + 2(1-\xi)(2-\xi)\frac{1}{yz} + \xi\frac{z}{y} \\ &\quad +(12-\xi)\frac{y}{z} + 2\xi\frac{y}{z^2} - \xi\frac{y^2}{z^2} - 4\frac{y^2}{z}\Bigg] \end{aligned} \tag{17}$$

$$H_F^4(y,z) = \frac{16\pi\alpha_s N_C C_F}{\sqrt{(1-y)^2-\xi}}\Bigg[-(4-5\xi)\frac{1}{y} - \xi(1-\xi)\left(\frac{1}{y^2}+\frac{1}{z^2}\right) -2(4-3\xi)\frac{1}{z} + \xi\frac{y}{z^2} + 2z + 2\frac{z}{y} + 6\frac{y}{z} - 2\frac{y^2}{z} + 2(1-\xi)(2-\xi)\frac{1}{yz}\Bigg] \quad (18)$$

In all three above expressions the denominator vanishes when the quark's three-momentum is zero, i.e. when $\vec{p}_1 = 0$ or, in terms of the y-variable, when $y = 1-\sqrt{\xi}$. However, a careful limiting procedure shows that the three structure functions in Eqs. (16)–(18) tend to finite limiting values (and not to zero as in the case of the longitudinal structure functions $H_L^{i\ell}$ treated in [3]). In contrast to this, the singularities at $y = z = 0$ constitute true IR-singularities. They can be regularized by introducing a small gluon mass $m_g = \sqrt{\Lambda q^2}$ which has the effect to deform the phase-space boundary to

$$y_- = \sqrt{\Lambda\xi} + \Lambda, \qquad y_+ = 1 - \sqrt{\xi} \quad (19)$$

$$z_\pm(y) = \frac{2y}{4y+\xi}\left\{1 - y - \frac{1}{2}\xi + \Lambda + \frac{\Lambda}{y} \pm \frac{1}{y}\sqrt{(y-\Lambda)^2 - \Lambda\xi}\sqrt{(1-y)^2-\xi}\right\}. \quad (20)$$

Note that the introduction of a small gluon mass is required only to deform the integration boundary. In the calculation of the matrix elements we need not pay regard to the gluon mass. With the gluon-mass regulator one can then perform the finite integration over the two phase-space variables y and z. The integration over z gives the cross section's dependence on the quark energy variable y. We obtain

$$\begin{aligned} H_F^{1\ell}(y) = \frac{8\pi\alpha_s N_C C_F}{(1-y)^2-\xi}\Bigg[& 2\Bigg\{2\frac{(1-\xi)(2-\xi)^2}{y} - 4(3-2\xi)(2-\xi) \\ & +(28-14\xi+\xi^2)y - 2(8-3\xi)y^2 + 4y^3\Bigg\}\ln\left(\frac{z_+(y)}{z_-(y)}\right) \\ & +\frac{1}{y}\sqrt{(y-\Lambda)^2-\Lambda\xi}\sqrt{(1-y)^2-\xi}\Bigg\{ -\frac{8\xi(1-\xi)(2-\xi)y}{\xi y^2 + 4\Lambda(1-y-\xi+\Lambda)} \\ & -8\frac{(1-\xi)(2-\xi)}{y} + 32(2-\xi) - 2(18-5\xi)y + 20y^2 \\ & -\frac{(4-\xi)(40+3\xi)y}{2(4y+\xi)} + \frac{(4-\xi)^3 y}{(4y+\xi)^2}\Bigg\}\Bigg] \end{aligned} \quad (21)$$

$$\begin{aligned} H_F^{2\ell}(y) = \frac{8\pi\alpha_s N_C C_F}{(1-y)^2-\xi}\,\xi\Bigg[& 2\Bigg\{2\frac{(1-\xi)(2-\xi)}{y} - 4(3-2\xi) \\ & +(12-\xi)y - 4y^2\Bigg\}\ln\left(\frac{z_+(y)}{z_-(y)}\right) \\ & +\frac{1}{y}\sqrt{(y-\Lambda)^2-\Lambda\xi}\sqrt{(1-y)^2-\xi}\Bigg\{ -\frac{8\xi(1-\xi)y}{\xi y^2 + 4\Lambda(1-y-\xi+\Lambda)} \end{aligned}$$

$$-8\frac{1-\xi}{y}+32-12y-4\frac{(4-\xi)y}{4y+\xi}\Big\}\Big] \tag{22}$$

$$\begin{aligned} H_F^4(y) &= \frac{16\pi\alpha_s N_C C_F}{\sqrt{(1-y)^2-\xi}}\Big[\,2\Big\{\frac{(1-\xi)(2-\xi)}{y}-(4-3\xi)+3y-y^2\Big\}\ln\left(\frac{z_+(y)}{z_-(y)}\right) \\ &\quad +\frac{1}{y}\sqrt{(y-\Lambda)^2-\Lambda\xi}\sqrt{(1-y)^2-\xi}\Big\{-\frac{4\xi(1-\xi)y}{\xi y^2+4\Lambda(1-y-\xi+\Lambda)} \\ &\quad -4\frac{1-\xi}{y}+8-y-\frac{16y}{4y+\xi}+\frac{(4-\xi)^2y}{(4y+\xi)^2}\Big\}\Big]. \end{aligned} \tag{23}$$

Let us briefly pause to discuss the y-dependence of the forward/backward (F)-polarization component P_F^ℓ which we define as the $(2\cos\theta)$-moment of the full θ-dependent polarization $P^\ell(\cos\theta)$, i.e.

$$\langle 2\cos\theta\, P^\ell(\cos\theta)\rangle = \frac{g_{41}H_F^{1\ell}+g_{42}H_F^{2\ell}}{g_{11}H_{U+L}^1+g_{12}H_{U+L}^2} =: P_F^\ell. \tag{24}$$

The IR-limit $y\to 0$ in Eq. (24) is well defined since the potentially singular term proportional to $1/y$ in the numerator is cancelled by the $1/y$-terms of the denominator giving a finite polarization value for $y\to 0$. In fact the limiting value of P_F^ℓ can be calculated to be

$$P_F^\ell(y\to 0)=\frac{2(2-\xi)g_{41}+2\xi g_{42}}{(4-\xi)g_{11}+3\xi g_{12}}. \tag{25}$$

Turning to the other corner of phase-space $y\to 1-\sqrt{\xi}$, the limiting value of the polarization expressions can be obtained by expanding numerator and denominator around $y=1-\sqrt{\xi}$. As mentioned before, the $(U+L)$- and (L)-components of the polarization vanish in this limit, whereas the (F)-component of the polarization tends to the finite limiting value

$$P_F^\ell(y\to 1-\sqrt{\xi})=-\frac{2((2-2\sqrt{\xi}-\xi)g_{41}+\xi g_{42})}{3((4-4\sqrt{\xi}+3\xi)g_{11}-\xi g_{12})}. \tag{26}$$

In Fig. 2 we have plotted the y-dependence of P_F^ℓ for the top quark case for the three values $\sqrt{q^2}=380$, 500 and 1000 GeV using a top quark mass of $m_t=180$ GeV [8].[‡] The polarization P_F^ℓ can be seen to tend to the two limiting values given in Eqs. (25) and (26) as $y\to 0$ and $y\to 1-\sqrt{\xi}$, respectively.

[‡]We have chosen the lowest energy $\sqrt{q^2}=380$ GeV to lie well above the nominal threshold value of $\sqrt{q^2}=360$ GeV for a perturbative calculation to make sense. As is well known, the production dynamics in the threshold region requires the consideration of non-perturbative effects. For a discussion of top quark polarization effects in the threshold region see [9].

Finally, with the integration over y we include the relative three-body/two-body phase-space factor $q^2/16\pi^2 v$ and express the result in terms of the rate functions

$$\hat{H}_\alpha^{i(\ell)}(tree) = \frac{q^2}{16\pi^2 v}\int dy\, dz\, H_\alpha^{i(\ell)}(y,z) \tag{27}$$

for $\alpha = F$, which gives

$$\begin{aligned}
\hat{H}_F^{1\ell}(tree) &= \frac{\alpha_s N_C C_F q^2}{2\pi v}\Big[\,(8-4\xi-\xi^2)J_1 - 2(2-\xi)(2-3\xi)J_2 \\
&\quad -\xi(1-\xi)(2-\xi)(J_3+J_9) - 2\xi J_4 - 4J_6 - 6\xi J_7 - 4(2-\xi)(3-2\xi)J_8 \\
&\quad +2(1-\xi)(2-\xi)^2 J_{10} + (4-2\xi-\xi^2)J_{11} + (28-14\xi+\xi^2)J_{12} \\
&\quad +2\xi(2-\xi)J_{13} - \xi(4-\xi)J_{14} + 4J_{15} + 2\xi J_{16} - 2(8-3\xi)J_{17}\Big]
\end{aligned} \tag{28}$$

$$\begin{aligned}
\hat{H}_F^{2\ell}(tree) &= \frac{\alpha_s N_C C_F q^2}{2\pi v}\,\xi\Big[\,(4+\xi)J_1 - 2(2-3\xi)J_2 - \xi(1-\xi)(J_3+J_9) \\
&\quad +4J_7 - 4(3-2\xi)J_8 + 2(1-\xi)(2-\xi)J_{10} + \xi J_{11} \\
&\quad +(12-\xi)J_{12} + 2\xi J_{13} - \xi J_{14} - 4J_{17}\Big]
\end{aligned} \tag{29}$$

$$\begin{aligned}
\hat{H}_F^{4}(tree) &= \frac{\alpha_s N_C C_F q^2}{\pi v}\Big[\,-(4-5\xi)S_2 - \xi(1-\xi)(S_3+S_5) - 2(4-3\xi)S_4 \\
&\quad +\xi S_6 + 2S_8 + 2S_9 + 6S_{10} - 2S_{11} + 2(1-\xi)(2-\xi)S_{12}\Big].
\end{aligned} \tag{30}$$

The integrals S_i have been computed and listed in [1]. Similar techniques allow one to calculate the integrals J_i (for details see [1,3]). They are listed in Appendix A. Remember that the IR-singularities in S_3, S_5, S_{12}, J_3, J_9 and J_{10} are cancelled by the corresponding IR-singularities of the virtual contributions. This is a consequence of the Lee-Nauenberg theorem.

3 Soft- and hard-gluon regions

For some applications it is desirable to split the three-body phase-space into a soft and a hard gluon region. The two regions are defined with respect to a fixed cut-off value of the gluon energy $E_g^{\text{cut-off}} = \lambda\sqrt{q^2}$ such that $E_g/\sqrt{q^2} \le \lambda$ and $E_g/\sqrt{q^2} > \lambda$ define the soft and the hard-gluon regions, respectively. Technically the integration over the soft-gluon region is quite simple. The hard-gluon contribution can then be obtained as the complement of

the soft-gluon contribution. Since we provide numerically stable expressions for both the total $O(\alpha_s)$ contribution and the soft-gluon contribution the computation of the hard-gluon contribution as the difference of the two constitutes a numerically stable procedure without that differences of large numbers are encountered.

In as much as the soft-gluon contribution factorizes into a Born term part and a universal soft-gluon function we begin our discussion by listing the relevant nonvanishing Born term components of the hadron tensor. One has

Born term:

$$\begin{aligned}
H_U^{4\ell} &= 4N_C q^2 v \\
H_L^{4\ell} &= 0 \\
H_F^{1\ell} &= 2N_C q^2(1+v^2) \qquad H_F^{2\ell} = 2N_C q^2(1-v^2) \\
H_U^1 &= 2N_C q^2(1+v^2) \qquad H_U^2 = 2N_C q^2(1-v^2) \\
H_L^1 &= N_C q^2(1-v^2) = H_L^2 \\
H_F^4 &= 4N_C q^2
\end{aligned} \tag{31}$$

where $v = \sqrt{1-4m^2/q^2}$ is the velocity of the quark in the c.m. system. For completeness we note that the polarized and unpolarized Born term cross sections can be obtained from Eqs. (11) and (12) by the replacement

$$\frac{d\sigma_\alpha^i}{dy\,dz} \;\rightarrow\; \sigma_\alpha^i = \frac{\pi\alpha^2 v}{3q^4} H_\alpha^i(Born) \tag{32}$$

and the same for the polarized cross sections.

Turning to the soft-gluon region of the $O(\alpha_s)$ tree-graph contribution, it is well-known that the soft hadronic tensor factorizes into the Born term structure times a universal function of the soft-gluon energy. Integrating the soft-gluon spectrum and adding the $O(\alpha_s)$ soft-gluon contribution to the Born term contribution, one obtains

$$\begin{aligned}
H_\alpha^i = H_\alpha^i(Born)\Bigg[1 - \frac{\alpha_s C_F}{\pi}\Bigg\{ &\ln\left(\frac{2\lambda}{\sqrt{\Lambda}}\right)\left(2 + \frac{1+v^2}{v}\ln\left(\frac{1-v}{1+v}\right)\right) \\
&+\frac{1}{v}\ln\left(\frac{1-v}{1+v}\right) + \frac{1+v^2}{v}\left(\mathrm{Li}_2\left(\frac{2v}{1+v}\right) + \frac{1}{4}\ln^2\left(\frac{1-v}{1+v}\right)\right)\Bigg\}\Bigg]
\end{aligned} \tag{33}$$

where the scaled maximal gluon energy λ denotes the cut-off energy which separates the soft-gluon region from the hard-gluon region. The IR singularity present in the soft-gluon

region has been regularized as before by introducing a small gluon mass $m_g = \sqrt{\Lambda q^2}$ which of course can be chosen to be arbitrarily small compared to the energy cut-off parameter λ.

The total $O(\alpha_s)$ soft-gluon contribution is then obtained by adding in the one-loop contribution. For the latter one has (see e.g. [1,3])

one-loop real part:

$$\begin{aligned}
H_U^{4\ell} &= 4N_C q^2 v(Re\,A + Re\,C) \\
H_L^{4\ell} &= 0 \\
H_F^{1\ell} &= 4N_C q^2(Re\,A + v^2\,Re\,C) \qquad H_F^{2\ell} = 4N_C q^2(Re\,A - v^2\,Re\,C) \\
H_U^{1} &= 4N_C q^2(Re\,A + v^2\,Re\,C) \qquad H_U^{2} = 4N_C q^2(Re\,A - v^2\,Re\,C) \\
H_L^{1} &= 2N_C q^2((1-v^2)\,Re\,A + v^2\,Re\,B) = H_L^2 \\
H_F^{4} &= 4N_C q^2 v(Re\,A + Re\,C)
\end{aligned} \tag{34}$$

one-loop imaginary part:

$$\begin{aligned}
H_U^{3\ell} &= -4N_C q^2 v(Im\,A - Im\,C) \\
H_L^{3\ell} &= 0 \\
H_F^{3} &= -4N_C q^2 v(Im\,A - Im\,C)
\end{aligned} \tag{35}$$

where the one-loop form factors A, B and C are given by

$$\begin{aligned}
Re\,A &= -\frac{\alpha_s C_F}{4\pi}\left[\left(2 + \frac{1+v^2}{v}\ln\left(\frac{1-v}{1+v}\right)\right)\ln\left(\frac{\Lambda q^2}{m^2}\right) + 3v\ln\left(\frac{1-v}{1+v}\right) + 4\right. \\
&\quad \left. + \frac{1+v^2}{v}\left(\mathrm{Li}_2\left(\frac{2v}{1+v}\right) + \frac{1}{4}\ln^2\left(\frac{1-v}{1+v}\right) - \frac{\pi^2}{2}\right)\right] \\
Re\,B &= \frac{\alpha_s C_F}{4\pi}\frac{1-v^2}{v}\ln\left(\frac{1-v}{1+v}\right) \qquad Re\,C = Re\,A - 2\,Re\,B \\
Im\,B &= \frac{\alpha_s C_F}{4\pi}\frac{1-v^2}{v}\pi \qquad Im\,C = Im\,A - 2\,Im\,B.
\end{aligned} \tag{36}$$

The γ_5-even one-loop results for $H_{U,L}^{1,2}$ and $H_{U,L}^{4\ell}$ are taken from [1,3]. The γ_5-odd one-loop contributions $H_F^{1\ell}$, $H_F^{2\ell}$ and H_F^4 have been calculated in dimensional regularization with zero gluon mass using a naive anticommuting γ_5. The result was then converted to the gluon mass regularization scheme with the help of the substitution
$1/\varepsilon - \gamma_E + \ln(4\pi\mu^2/m^2) \to \ln(\Lambda q^2/m^2)$.

Although the imaginary part of the one-loop contribution is only needed in the case of transverse normal polarization (see [4]), we have included it for completeness. It is quite apparent that the sum of the real gluon emission contributions in Eq. (33) and the real one-loop contributions in Eq. (34) are IR finite, i.e. the dependence on Λ drops out in the sum.

We have numerically evaluated the polarization in the soft-gluon region as a function of the gluon energy cut-off. We did not plot the results since the $O(\alpha_s)$ corrections to the polarization are quite small. In the scale of our figures the corrections only become visible for $\lambda < 0.1\%$ which is too low a cut-off-value for a fixed order perturbation series to make sense. In fact, the unpolarized $O(\alpha_s)$ rate crosses zero and becomes negative at around $\lambda = 0.05\%$ which again highlights the fact that such low cut-off values do not make any sense. One concludes that the $O(\alpha_s)$ corrections go in the same direction for both polarized and unpolarized rates rendering the ratio unsensitive to $O(\alpha_s)$ corrections.

Let us now present our results for the fully integrated three-body tree-graph polarized rate functions in terms of the rate functions given in Eq. (27). As mentioned before, we integrate over the full phase-space keeping a small gluon mass as IR-cutoff. The complete $O(\alpha_s)$ contribution is then given by adding in the $O(\alpha_s)$ real one-loop contributions listed in Eq. (34). One has

$$\hat{H}^{i\ell}_{\alpha}(\alpha_s) = \hat{H}^{i\ell}_{\alpha}(tree) + H^{i\ell}_{\alpha}(loop). \tag{37}$$

Note that the dependence on the IR-cutoff parameter Λ drops out in the sum of the two contributions. One has

$O(\alpha_s)$ *real part:*

$$\begin{aligned}\hat{H}^{4\ell}_{U}(\alpha_s) &= \frac{\alpha_s N_C C_F q^2}{4\pi v}\Big[-2(1-\sqrt{\xi})(2-6\sqrt{\xi}+29\xi) - 16v^2 t_{11} - 16v^2 t_{10} \\ &\quad +8(2-\xi)v(t_7-t_8) - 2(8+2\xi+3\xi^2)t_6 + 4(4+9\xi)vt_3 \\ &\quad -(16-30\xi+\frac{17}{2}\xi^2)(t_1-t_2)\Big] \end{aligned} \tag{38}$$

$$\begin{aligned}\hat{H}^{4\ell}_{L}(\alpha_s) &= \frac{\alpha_s N_C C_F q^2}{4\pi v}\Big[4(1-\sqrt{\xi})(2-6\sqrt{\xi}+13\xi) + 2\xi(10+3\xi)t_6 \\ &\quad -52\xi v t_3 - \xi(24-7\xi)(t_1-t_2)\Big] \end{aligned} \tag{39}$$

$$\hat{H}_F^{1\ell}(\alpha_s) = \frac{\alpha_s N_C C_F q^2}{4\pi v}\Big[-4(2+3\xi)v - 16(2-\xi)vt_{12} - 8(2-\xi)vt_{10} \\ -4(2-\xi)^2(t_8-t_9) + 2\xi(10-\xi)t_5 + 2\sqrt{\xi}(1-\sqrt{\xi})(2-\sqrt{\xi})(4+\sqrt{\xi})t_4 \\ +2(24-12\xi+\xi^2)t_3 \Big] \tag{40}$$

$$\hat{H}_F^{2\ell}(\alpha_s) = \frac{\alpha_s N_C C_F q^2}{4\pi v}\xi\Big[12v - 16vt_{12} - 8vt_{10} - 4(2-\xi)(t_8-t_9) \\ +2\xi t_5 + 2\sqrt{\xi}(1-\sqrt{\xi})t_4 + 2(6-\xi)t_3 \Big] \tag{41}$$

$$\hat{H}_U^1(\alpha_s) = \frac{\alpha_s N_C C_F q^2}{4\pi v}\Big[2(2+7\xi)v - 16(2-\xi)vt_{12} - 8(2-\xi)vt_{10} - 4(2-\xi)^2(t_8-t_9) \\ -2\xi(2+3\xi)t_5 + 2\sqrt{\xi}(1-\sqrt{\xi})(2+4\sqrt{\xi}-3\xi)t_4 + (48-48\xi+7\xi^2)t_3 \Big] \tag{42}$$

$$\hat{H}_U^2(\alpha_s) = \frac{\alpha_s N_C C_F q^2}{4\pi v}\xi\Big[12v - 16vt_{12} - 8vt_{10} - 4(2-\xi)(t_8-t_9) \\ +2\xi t_5 + 2\sqrt{\xi}(1-\sqrt{\xi})t_4 + 2(6-\xi)t_3 \Big] \tag{43}$$

$$\hat{H}_L^1(\alpha_s) = \frac{\alpha_s N_C C_F q^2}{4\pi v}\Big[(8-23\xi+\frac{3}{2}\xi^2)v - 8\xi vt_{12} - 4\xi vt_{10} - 2\xi(2-\xi)(t_8-t_9) \\ +2\xi(2+3\xi)t_5 - 2\sqrt{\xi}(1-\sqrt{\xi})(2+4\sqrt{\xi}-3\xi)t_4 \\ +\xi(22-8\xi+\frac{3}{4}\xi^2)t_3 \Big] \tag{44}$$

$$\hat{H}_L^2(\alpha_s) = \frac{\alpha_s N_C C_F q^2}{4\pi v}\xi\Big[\frac{3}{2}(10-\xi)v - 8vt_{12} - 4vt_{10} - 2(2-\xi)(t_8-t_9) \\ -2\xi t_5 - 2\sqrt{\xi}(1-\sqrt{\xi})t_4 + (6-4\xi-\frac{3}{4}\xi^2)t_3 \Big] \tag{45}$$

$$\hat{H}_F^4(\alpha_s) = \frac{\alpha_s N_C C_F q^2}{4\pi v}\Big[-16\sqrt{\xi}(1-\sqrt{\xi}) - 16v^2t_{11} - 16v^2t_{10} \\ +8(2-\xi)v(t_7-t_8) - 4(4-5\xi)t_6 + 8(2-3\xi)vt_3 - 16(t_1-t_2) \Big] \tag{46}$$

Closed form expressions for the $O(\alpha_s)$ rate functions t_i ($i = 1, \ldots, 12$) appearing in Eqs. (38)–(46) can be found in Appendix B. They contain the set of basic I, J, S and T integrals calculated in [1] (I, S), [3] (T) and in Appendix A (J). They are associated with the various hadron tensor components in the following way: $U(S,T)$, $L(T)$, $[U+L](S)$ and $F(J)$ (polarized case) and $U(I,J)$, $L(J)$, $[U+L](I)$ and $F(S)$ (unpolarized case). We mention that, concerning the unpolarized (F)-component in Eq. (46), closed form expressions for this component are also given in [10] and [11]. We agree with the results of these authors.

For our numerical evaluation we take the current world mean value for α_s, i.e.

$\alpha_s(M_Z) = 0.118$ for five active flavours and evolve α_s by use of the one-loop renormalization group equation. For the bottom and top mass we use pole mass values $m_b = 4.83$ GeV [12] and $m_t = 180$ GeV [8]. We have repeated the numerical evaluation using $\overline{\rm MS}$ running masses $\bar{m}_b(\bar{m}_b) = 4.44$ GeV and $\bar{m}_t(\bar{m}_t) = 172.1$ GeV where the running of the masses follows the momentum dependence of the corresponding one-loop renormalization group equation [13]. However, since the polarization expressions are rather insensitive to which sets of masses is used, our numerical results in Figs. 2 and 3 are given only in terms of the above pole masses.

In Fig. 3 we show the polar angle dependence of the alignment polarization of top quarks in the continuum, and for bottom quarks on the Z. We want to emphasize that we define the $O(\alpha_s)$ polarization such that we keep the full $O(\alpha_s)$ dependence of the unpolarized rate functions in the denominator. Thus we do not expand the inverse of the rate functions in powers of α_s as is sometimes done in the literature.

The $\cos\theta$-dependence of the alignment polarization of the top quark shown in Fig. 3a is quite strong for all three c.m. energies 380 GeV, 500 GeV and 1000 GeV and shows a strong forward-backward asymmetry signalling a strong (F)-component in the polarization. The energy dependence of the alignment polarization is not very pronounced where the asymmetry becomes somewhat larger as the energy increases. Shown are the full $O(\alpha_s)$ results for the polarization. We did not plot the corresponding Born term results since the respective $O(\alpha_s)$ and Born term results differ by less than 2% in absolute value. Again the $O(\alpha_s)$ corrections in the numerator and in the denominator of the polarization expression tend to go in the same direction leaving the polarization practically unchanged under $O(\alpha_s)$ corrections. For the bottom quark case shown in Fig. 3b we plot the Born term results and the full $O(\alpha_s)$ results separately. Note, however, that the $O(\alpha_s)$ corrections amount to only $\cong 2\%$ over the whole $\cos\theta$ range. In order to be able to exhibit the size of the $O(\alpha_s)$ corrections we chose to use a "suppressed zero" plot in Fig. 3b. The $\cos\theta$ dependence of the alignment polarization is very weak with a small asymmetry component. We have checked that using a running mass $\bar{m}_b(M_z) = 3.30$ GeV in Fig. 3b changes the results by less than 0.2%.

4 Massless QCD and the zero-mass limit of QCD

It is well known by now that, as concerns spin-flip contributions induced by gluon radiation, the zero-mass limit of QCD and massless QCD do not coincide, at least in the perturbative sector [1,2,3,14,15]. Since familiarity with this statement is not so widespread we want to use this section to highlight the difference between the $m = 0$ and $m \to 0$ $O(\alpha_s)$ results for the alignment polarization. Needless to say that this has important practical implications for the calculation of polarization observables for the process $Z \to$ *light quark-pairs* where one might be tempted to set the quark mass to zero from the very beginning because of the presence of the large Z-mass scale.

Let us begin our discussion by listing the zero-mass Born term contributions. These are

$$H_U^{4\ell} \;=\; H_U^1 \;=\; H_F^{1\ell} \;=\; H_F^4 \;=\; 4N_C q^2 \tag{47}$$

$$H_L^{4\ell} \;=\; H_L^1 \;=\; 0. \tag{48}$$

Next we write down the $O(\alpha_s)$ zero-mass tree-graph contributions, which read

$$H_{U+L}^{4\ell}(y,z) \;=\; H_{U+L}^1(y,z) \;=\; 32\pi\alpha_s N_C C_F\, \frac{(1-y)^2+(1-z)^2}{yz} \tag{49}$$

$$H_L^{4\ell}(y,z) \;=\; H_L^1(y,z) \;=\; 32\pi\alpha_s N_C C_F\, \frac{2(1-y-z)}{(1-y)^2} \tag{50}$$

$$H_F^{1\ell}(y,z) \;=\; H_F^4(y,z) \;=\; 32\pi\alpha_s N_C C_F \left(\frac{(1-y)^2+(1-z)^2}{yz} - 2\,\frac{1-z}{1-y}\right). \tag{51}$$

Note that for massless QCD one has $H_\alpha^2 = H_\alpha^{2\ell} = 0$ and $H_\alpha^3 = H_\alpha^{3\ell} = 0$ to any order in α_s. This is implicit in the following discussion.

The hadron tensors H_α ($\alpha = U+L, F$) become singular for $y \to 1$ and $z \to 1$. These singularities need to be regularized when integrating over (y,z) phase space. A particularly convenient regularization scheme is regularization by dimensional reduction [16] where the spin degrees of freedom are kept in four dimensions and only scalar integrals are regularized dimensionally. In this scheme one can retain the matrix element expressions Eq. (49–51) when doing the n-dimensional phase space integration. After adding in the loop contribution (also regularized by dimensional reduction) the finite result can be

transposed to the dimensional regularization scheme by adding in a finite global counter-term [17] which will be specified later on. The dimensional reduction calculation of the rates proceeds along the lines discussed in [18].

The tree-graph expressions have to be integrated with respect to the n-dimensional integration measure ($n = 4 - 2\varepsilon$)

$$\frac{q^2}{16\pi^2}\left(\frac{4\pi\mu^2}{q^2}\right)^{\varepsilon}\frac{1}{\Gamma(1-\varepsilon)}\int_0^1 dy\int_0^{1-y} dz\, y^{-\varepsilon}z^{-\varepsilon}(y+z-1)^{-\varepsilon} \tag{52}$$

where we have again included the relative two-body/three-body phase-space factor $q^2/16\pi^2$ as before ($v = 1$ for massless quarks).

The integrations can be done in standard fashion, and one obtains the tree-graph contributions

$$\hat{H}^{4\ell}_{U+L}(tree) \;=\; \hat{H}^{1}_{U+L}(tree) \;=\; 4N_C q^2\frac{\alpha_s}{\pi}C_F C\left(\frac{1}{\varepsilon^2}+\frac{3}{2\varepsilon}+\frac{17}{4}\right) \tag{53}$$

$$\hat{H}^{4\ell}_{L}(tree) \;=\; \hat{H}^{1}_{L}(tree) \;=\; 4N_C q^2\frac{\alpha_s}{\pi}C_F C\left(\frac{1}{2}\right) \tag{54}$$

$$\hat{H}^{1\ell}_{F}(tree) \;=\; \hat{H}^{4}_{F}(tree) \;=\; 4N_C q^2\frac{\alpha_s}{\pi}C_F C\left(\frac{1}{\varepsilon^2}+\frac{3}{2\varepsilon}+\frac{17}{4}-\frac{3}{4}\right) \tag{55}$$

where

$$C = \left(\frac{4\pi\mu^2}{q^2}\right)^{\varepsilon}\frac{\Gamma^2(1-\varepsilon)}{\Gamma(1-3\varepsilon)}. \tag{56}$$

The right-most finite contributions in the round bracket of Eq. (55) results from the integration of the right-most term in the round bracket of Eq. (51).

The loop contributions in dimensional reduction are given by ($H^{4\ell}_L = H^1_L = 0$) [18]

$$H^{4\ell}_U = H^1_U = H^{1\ell}_F = H^4_F = 4N_C q^2\frac{\alpha_s}{\pi}C_F C'\left(-\frac{1}{\varepsilon^2}-\frac{3}{2\varepsilon}-3\right) \tag{57}$$

where one has to remember to do all γ-matrix manipulations in four dimensions. C' is given by

$$C' = \left(\frac{4\pi\mu^2}{-q^2}\right)^{\varepsilon}\frac{\Gamma(1+\varepsilon)\Gamma^2(1-\varepsilon)}{\Gamma(1-2\varepsilon)}. \tag{58}$$

For the real parts that are of interest here we have $C' = C + O(\varepsilon^3)$.

In order to convert our results to the more familiar dimensional regularization result we have to add the global counter-term, which reads ($H^{4\ell}_L = H^1_L = 0$) [17]

$$H^{4\ell}_U = H^1_U = H^{1\ell}_F = H^4_F = 4N_C q^2\frac{\alpha_s}{\pi}C_F\left(-\frac{1}{2}\right). \tag{59}$$

By adding up all the contributions including the counter-term we arrive at the full $O(\alpha_s)$ result

$$\hat{H}_U^{4\ell}(\alpha_s) = \hat{H}_U^1(\alpha_s) = 4N_C q^2 \frac{\alpha_s}{\pi} C_F \left(\frac{1}{4}\right) \tag{60}$$

$$\hat{H}_L^{4\ell}(\alpha_s) = \hat{H}_L^1(\alpha_s) = 4N_C q^2 \frac{\alpha_s}{\pi} C_F \left(\frac{1}{2}\right) \tag{61}$$

$$\hat{H}_F^{1\ell}(\alpha_s) = \hat{H}_F^4(\alpha_s) = 0. \tag{62}$$

For easy reference one may add the Born term contribution to obtain the familiar result ($C_F = 4/3$) $H_{U+L}^1 = 4N_C q^2(1 + \alpha_s/\pi)$. The vanishing of H_F^4 and thereby $H_F^{1\ell}$ in massless QCD has been noted before [7,19].[§]

As it turns out one does not reproduce the polarized result in Eq. (60) and in Eq. (62) when taking the $m \to 0$ limit in the corresponding expressions Eqs. (38) and (40) in Sec. 3, respectively. One obtains instead

$$\hat{H}_U^{4\ell}(\alpha_s) = 4N_C q^2 \frac{\alpha_s}{\pi} C_F \left(\frac{1}{4} - \left[\frac{1}{2}\right]\right) \tag{63}$$

$$\hat{H}_F^{4\ell}(\alpha_s) = 4N_C q^2 \frac{\alpha_s}{\pi} C_F \left(\frac{1}{2}\right) \tag{64}$$

$$\hat{H}_F^{1\ell}(\alpha_s) = 4N_C q^2 \frac{\alpha_s}{\pi} C_F \left(0 - \left[\frac{1}{2}\right]\right) \tag{65}$$

where, by hindsight, we have split the contributions in the round brackets into a normal spin non-flip piece and an anomalous spin-flip piece. Note the drastic changes in the $O(\alpha_s)$ results for $H_U^{4\ell}$ and $H_F^{1\ell}$ when the anomalous pieces are included.

The anomalous spin-flip contributions have their origin in the collinear limit where the spin-flip contribution proportional to m survives since it is multiplied by the $1/m$ collinear mass singularity. Because the anomalous spin-flip terms are associated with the collinear singularity, the flip contributions are universal and factorize into the Born

[§]For a careful discussion of the γ_5-subtleties in dimensional regularization when deriving the zero result $\hat{H}_F^4(\alpha_s) = 0$ we refer the reader to [19]. In dimensional reduction the troublesome γ_5-odd traces can be completely avoided by deriving the cross section expression Eq.(51) and the one-loop contribution Eq.(57) in a well-defined manner by use of e.g. helicity amplitudes in which the massless axial vector current helicity amplitudes are related to the massless vector current helicity amplitudes in canonical fashion. This is implicit in Eq. (57) where we have used the relation $H_F^{1\ell} = H_F^4 = H_U^1 = H_U^{4\ell}$ to relate the troublesome γ_5-odd objects $H_F^{1\ell} = H_F^4$ to the unproblematic γ_5-even objects $H_U^{4\ell}$, H_U^1 using parity and γ_5-invariance.

term contribution and an universal spin-flip bremsstrahlung function [15]. This explains why there is no anomalous contribution to $H_L^{4\ell}$ and why the anomalous flip contributions to $H_U^{4\ell}$ and $H_F^{1\ell}$ are equal. In fact the strength of the anomalous spin-flip contribution can directly be calculated from the universal helicity-flip bremsstrahlung function listed in [15]. One has

$$\frac{dH_{hf}}{dy} = H(Born)\frac{\alpha_s}{2\pi}C_{_F}y \tag{66}$$

where y is the energy fraction of the quark after the radiative flip transition relative to that of the radiating quark ($0 \leq y \leq 1$). Integrating over y one finds

$$\int_0^1 dy\ \frac{dH_{hf}}{dy} = H(Born)\frac{\alpha_s}{2\pi}C_{_F}\,\frac{1}{2}. \tag{67}$$

Then considering the fact that the flip contribution contributes negatively to the alignment polarization (see Eq. (8)), and that there can be a flip on the antiquark side also, one reproduces exactly the anomalous flip contributions in Eqs. (63) and (65).

It is important to realize that the anomalous spin flip contribution does not come into play when calculating the transverse polarization of a single quark, because of the extra $m/\sqrt{q^2}$ factor in the transverse polarization expressions. However, when calculating quark-antiquark polarization correlation effects, the $O(\alpha_s)$ anomalous contribution does come in even when considering transverse polarization effects.

5 Summary and Conclusion

We have presented the results of an $O(\alpha_s)$ calculation of the full polar angle dependence of the quark's alignment polarization with respect to the electron beam direction including beam polarization effects. This completes a series of papers devoted to the full calculation of quark polarization effects on and off the Z-peak in e^+e^--annihilations into a pair of massive quarks. When averaged over phase-space, the $O(\alpha_s)$ corrections to the polarization observables are generally small (typically of the order 2%) indicating that the $O(\alpha_s)$ corrections to the polarized and unpolarized rates tend to go in the same direction. This of course must not be true everywhere in phase-space and for every polarization component. We mention that our results are also of relevance for the final-state radiative QED

corrections to lepton polarization in $e^+e^- \to \tau^+\tau^-$ [20], where, to our knowledge, a full $O(\alpha)$ calculation including quark mass effects has not yet been published.

We have not discussed how to measure the polarization of the quarks either when it decays as a free quark as in top quarks, or when it decays as a bound quark in e.g. polarized Λ_b-baryon decays. There exist a long list of papers devoted to this subject, among which are the papers listed in [21,22]. Of particular interest is the transverse normal polarization studied in [4,22,23,24]. It provides the SM background to possible CP-violating contributions to transverse polarization considered in [23,24]. In fact, by comparing the transverse normal polarization of the quark and the antiquark, the truly CP-violating contributions can be separated [24].

Recently there has been a thorough numerical study of gluonic corrections to top quark pair production *and* decay (interference effects not included) [25]. By using helicity amplitudes for both the production and decay process, the full spin momentum correlation structure of the production and decay process has been retained in the calculation of [25]. The production-side information in [25] is identical to the information contained in our paper. However, we believe that our results are physically more transparent since we have chosen a two-step approach in which we first represent the production-side dynamics in terms of the polarization components of the produced top quarks including beam polarization effects as in [25]. The polarization of the produced top quarks can then be probed by its subsequent decay. Also, by using analytical methods, we were able to effect large rate cancellations in sensitive areas of phase-space. These could lead to numerically unstable results in the purely numerical approach of [25] when not properly dealt with. At any rate, by comparing the production-side results of [25] and our results one has a powerful check on the technically rather involved calculation of gluonic corrections to the polarization of quarks in e^+e^--annihilation.

Acknowledgement: We would like to thank D.H. Schiller for allowing us to freely quote from the unpublished material in [26] when writing Appendix C.

Appendix A

The list of J-integrals appearing in Section 2 had been calculated completely by an uniform substitution. The substitution $1-y=\sqrt{\xi}(1+\eta^2)/(1-\eta^2)$ leads to the replacement of the lower boundary $y=0$ by $\eta=w:=\sqrt{(1-\sqrt{\xi})/(1+\sqrt{\xi})}$, which occurs in most of the expressions. Remember also that we have $v=\sqrt{1-\xi}$.

$$\begin{aligned} J_1 &= \int \frac{dy\,dz}{(1-y)^2-\xi} \\ &= 2\,\frac{1-\xi}{4-\xi}\ln\left(\frac{1+v}{1-v}\right) \end{aligned} \tag{A1}$$

$$\begin{aligned} J_2 &= \int \frac{dy\,dz}{(1-y)^2-\xi}\;\frac{1}{y} \\ &= \frac{6}{4-\xi}\ln\left(\frac{1+v}{1-v}\right) \end{aligned} \tag{A2}$$

$$\begin{aligned} J_3 &= \int \frac{dy\,dz}{(1-y)^2-\xi}\;\frac{1}{y^2} \\ &= \frac{4}{\xi\,v}\left[-\ln\Lambda^{\frac{1}{2}}-\ln\xi+2\ln v+2\ln 2-1\right]-\frac{24}{\xi(4-\xi)}\ln\left(\frac{1+v}{1-v}\right) \end{aligned} \tag{A3}$$

$$\begin{aligned} J_4 &= \int \frac{dy\,dz}{(1-y)^2-\xi}\;y \\ &= -\left(1+\tfrac{1}{2}\xi-\frac{6}{4-\xi}\right)\ln\left(\frac{1+v}{1-v}\right)-v \end{aligned} \tag{A4}$$

$$\begin{aligned} J_5 &= \int \frac{dy\,dz}{(1-y)^2-\xi}\;y^2 \\ &= \left(2+\tfrac{1}{2}\xi+\tfrac{1}{8}\xi^2-\frac{6}{4-\xi}\right)\ln\left(\frac{1+v}{1-v}\right)-\tfrac{1}{4}(6-\xi)v \end{aligned} \tag{A5}$$

$$\begin{aligned} J_6 &= \int \frac{dy\,dz}{(1-y)^2-\xi}\;yz \\ &= \tfrac{1}{2}\xi\left(-2+\tfrac{1}{8}\xi+\frac{9}{4-\xi}-\frac{12}{(4-\xi)^2}\right)\ln\left(\frac{1+v}{1-v}\right)+\left(\tfrac{3}{4}+\tfrac{1}{8}\xi-\frac{2}{4-\xi}\right)v \end{aligned} \tag{A6}$$

$$\begin{aligned} J_7 &= \int \frac{dy\,dz}{(1-y)^2-\xi}\;z \\ &= -\frac{3\xi}{4-\xi}\left(1-\frac{2}{4-\xi}\right)\ln\left(\frac{1+v}{1-v}\right)+\frac{2v}{4-\xi} \end{aligned} \tag{A7}$$

$$
\begin{aligned}
J_8 &= \int \frac{dy\,dz}{(1-y)^2-\xi}\ \frac{1}{z} \\
&= \frac{1}{\sqrt{\xi}}\left[\,\mathrm{Li}_2(w)-\mathrm{Li}_2(-w)+\mathrm{Li}_2\left(\frac{2+\sqrt{\xi}}{2-\sqrt{\xi}}\,w\right)-\mathrm{Li}_2\left(-\frac{2+\sqrt{\xi}}{2-\sqrt{\xi}}\,w\right)\right] \qquad \text{(A8)}
\end{aligned}
$$

$$
\begin{aligned}
J_9 &= \int \frac{dy\,dz}{(1-y)^2-\xi}\ \frac{1}{z^2} \\
&= \frac{4}{\xi\,v}\left[-\ln\Lambda^{\frac{1}{2}}-\ln\xi+2\ln v+2\ln 2-\frac{2-\xi}{2v}\ln\left(\frac{1+v}{1-v}\right)\right] \qquad \text{(A9)}
\end{aligned}
$$

$$
\begin{aligned}
J_{10} &= \int \frac{dy\,dz}{(1-y)^2-\xi}\ \frac{1}{yz} \\
&= \frac{1}{2(1-\xi)}\ln\left(\frac{1+v}{1-v}\right)\Big[-4\ln\Lambda^{\frac{1}{2}}-\tfrac{5}{2}\ln\xi+5\ln(1+\sqrt{\xi})+4\ln(1-\sqrt{\xi}) \\
&\qquad\qquad -\ln(2+\sqrt{\xi})+6\ln 2\Big] \\
&\quad +\frac{2}{1-\xi}\left[\,\mathrm{Li}_2\left(\frac{1+v}{2}\right)-\mathrm{Li}_2\left(\frac{1-v}{2}\right)\right]+\frac{3}{1-\xi}\left[\,\mathrm{Li}_2\left(-\frac{2v}{1-v}\right)-\mathrm{Li}_2\left(\frac{2v}{1+v}\right)\right] \\
&\quad +\frac{1}{\sqrt{\xi}(1-\sqrt{\xi})}\left[\,\mathrm{Li}_2(w)-\mathrm{Li}_2(-w)+\mathrm{Li}_2\left(\frac{2+\sqrt{\xi}}{2-\sqrt{\xi}}\,w\right)-\mathrm{Li}_2\left(-\frac{2+\sqrt{\xi}}{2-\sqrt{\xi}}\,w\right)\right] \\
&\quad -\frac{1}{1-\xi}\Big[\mathrm{Li}_2\left(\frac{1+w}{2}\right)-\mathrm{Li}_2\left(\frac{1-w}{2}\right)+\mathrm{Li}_2\left((2+\sqrt{\xi})\frac{1+w}{4}\right) \\
&\quad -\mathrm{Li}_2\left((2+\sqrt{\xi})\frac{1-w}{4}\right)+\mathrm{Li}_2\left(\frac{2\sqrt{\xi}}{(2+\sqrt{\xi})(1+w)}\right)-\mathrm{Li}_2\left(\frac{2\sqrt{\xi}}{(2+\sqrt{\xi})(1-w)}\right)\Big] \qquad \text{(A10)}
\end{aligned}
$$

$$
\begin{aligned}
J_{11} &= \int \frac{dy\,dz}{(1-y)^2-\xi}\ \frac{z}{y} \\
&= \left(-1+\frac{12}{4-\xi}-\frac{24}{(4-\xi)^2}\right)\ln\left(\frac{1+v}{1-v}\right)-\frac{2v}{4-\xi} \qquad \text{(A11)}
\end{aligned}
$$

$$
\begin{aligned}
J_{12} &= \int \frac{dy\,dz}{(1-y)^2-\xi}\ \frac{y}{z} \\
&= \tfrac{1}{2}\ln\left(\frac{1+v}{1-v}\right)\left[\,\tfrac{1}{2}\ln\xi+\ln(2+\sqrt{\xi})-\ln(1+\sqrt{\xi})-2\ln 2\right] \\
&\quad +\frac{1-\sqrt{\xi}}{\sqrt{\xi}}\left[\,\mathrm{Li}_2(w)-\mathrm{Li}_2(-w)+\mathrm{Li}_2\left(\frac{2+\sqrt{\xi}}{2-\sqrt{\xi}}\,w\right)-\mathrm{Li}_2\left(-\frac{2+\sqrt{\xi}}{2-\sqrt{\xi}}\,w\right)\right] \\
&\quad +\mathrm{Li}_2\left(\frac{1+w}{2}\right)-\mathrm{Li}_2\left(\frac{1-w}{2}\right)+\mathrm{Li}_2\left((2+\sqrt{\xi})\frac{1+w}{4}\right)-\mathrm{Li}_2\left((2+\sqrt{\xi})\frac{1-w}{4}\right) \\
&\quad +\mathrm{Li}_2\left(\frac{2\sqrt{\xi}}{(2+\sqrt{\xi})(1+w)}\right)-\mathrm{Li}_2\left(\frac{2\sqrt{\xi}}{(2+\sqrt{\xi})(1-w)}\right) \qquad \text{(A12)}
\end{aligned}
$$

$$
\begin{aligned}
J_{13} &= \int \frac{dy\,dz}{(1-y)^2-\xi}\ \frac{y}{z^2} \\
&= \frac{2}{\xi}\ln\left(\frac{1+v}{1-v}\right) \qquad \text{(A13)}
\end{aligned}
$$

$$
\begin{aligned}
J_{14} &= \int \frac{dy\,dz}{(1-y)^2-\xi}\ \frac{y^2}{z^2} \\
&= \frac{2}{\xi}\left(\ln\left(\frac{1+v}{1-v}\right)-2v\right) \qquad \text{(A14)}
\end{aligned}
$$

$$
\begin{aligned}
J_{15} &= \int \frac{dy\,dz}{(1-y)^2-\xi}\ \frac{y^3}{z} \\
&= \tfrac{1}{2}(3+\xi)\ln\left(\frac{1+v}{1-v}\right)\left[\tfrac{1}{2}\ln\xi+\ln(2+\sqrt{\xi})-\ln(1+\sqrt{\xi})-2\ln 2\right] \\
&\quad +\frac{(1-\sqrt{\xi})^3}{\sqrt{\xi}}\left[\mathrm{Li}_2(w)-\mathrm{Li}_2(-w)+\mathrm{Li}_2\left(\frac{2+\sqrt{\xi}}{2-\sqrt{\xi}}\,w\right)-\mathrm{Li}_2\left(-\frac{2+\sqrt{\xi}}{2-\sqrt{\xi}}\,w\right)\right] \\
&\quad +(3+\xi)\Bigg[\mathrm{Li}_2\left(\frac{1+w}{2}\right)-\mathrm{Li}_2\left(\frac{1-w}{2}\right)+\mathrm{Li}_2\left((2+\sqrt{\xi})\frac{1+w}{4}\right) \\
&\quad -\mathrm{Li}_2\left((2+\sqrt{\xi})\frac{1-w}{4}\right)+\mathrm{Li}_2\left(\frac{2\sqrt{\xi}}{(2+\sqrt{\xi})(1+w)}\right)-\mathrm{Li}_2\left(\frac{2\sqrt{\xi}}{(2+\sqrt{\xi})(1-w)}\right)\Bigg] \\
&\quad +\frac{40-16\xi+\xi^2}{16}\ln\left(\frac{1+v}{1-v}\right)-\frac{26-\xi}{8}\,v \qquad \text{(A15)}
\end{aligned}
$$

$$
\begin{aligned}
J_{16} &= \int \frac{dy\,dz}{(1-y)^2-\xi}\ \frac{y^3}{z^2} \\
&= \frac{2+\xi}{\xi}\ln\left(\frac{1+v}{1-v}\right)-\frac{6}{\xi}v \qquad \text{(A16)}
\end{aligned}
$$

$$
\begin{aligned}
J_{17} &= \int \frac{dy\,dz}{(1-y)^2-\xi}\ \frac{y^2}{z} \\
&= \tfrac{1}{2}\ln\left(\frac{1+v}{1-v}\right)\left[\tfrac{1}{2}\ln\xi+\ln(2+\sqrt{\xi})-\ln(1+\sqrt{\xi})-2\ln 2\right] \\
&\quad +\frac{(1-\sqrt{\xi})^2}{\sqrt{\xi}}\left[\mathrm{Li}_2(w)-\mathrm{Li}_2(-w)+\mathrm{Li}_2\left(\frac{2+\sqrt{\xi}}{2-\sqrt{\xi}}\,w\right)-\mathrm{Li}_2\left(-\frac{2+\sqrt{\xi}}{2-\sqrt{\xi}}\,w\right)\right] \\
&\quad +\mathrm{Li}_2\left(\frac{1+w}{2}\right)-\mathrm{Li}_2\left(\frac{1-w}{2}\right)+\mathrm{Li}_2\left((2+\sqrt{\xi})\frac{1+w}{4}\right) \\
&\quad -\mathrm{Li}_2\left((2+\sqrt{\xi})\frac{1-w}{4}\right)+\mathrm{Li}_2\left(\frac{2\sqrt{\xi}}{(2+\sqrt{\xi})(1+w)}\right)-\mathrm{Li}_2\left(\frac{2\sqrt{\xi}}{(2+\sqrt{\xi})(1-w)}\right) \\
&\quad +\frac{2-\xi}{2}\ln\left(\frac{1+v}{1-v}\right)-v \qquad \text{(A17)}
\end{aligned}
$$

Appendix B

It is convenient to define the mass dependent variables $a := 2+\sqrt{\xi}$, $b := 2-\sqrt{\xi}$ and $w := \sqrt{(1-\sqrt{\xi})/(1+\sqrt{\xi})}$. The functions $t_1, \ldots, t_{12}$ appearing in Eqs. (38)–(46) are then given by

$$t_1 := \ln\left(\frac{2\xi\sqrt{\xi}}{b^2(1+\sqrt{\xi})}\right), \quad t_2 := \ln\left(\frac{2\sqrt{\xi}}{1+\sqrt{\xi}}\right) \quad \Rightarrow \quad t_1 - t_2 = \ln\left(\frac{\xi}{b^2}\right) \tag{B1}$$

$$t_3 := \ln\left(\frac{1+v}{1-v}\right) \tag{B2}$$

$$t_4 := \mathrm{Li}_2(w) - \mathrm{Li}_2(-w) + \mathrm{Li}_2(\frac{a}{b}w) - \mathrm{Li}_2(-\frac{a}{b}w) \tag{B3}$$

$$\begin{aligned} t_5 := {} & \frac{1}{2}\ln\left(\frac{a\sqrt{\xi}}{4(1+\sqrt{\xi})}\right)\ln\left(\frac{1+v}{1-v}\right) + \mathrm{Li}_2\left(\frac{2\sqrt{\xi}}{a(1+w)}\right) - \mathrm{Li}_2\left(\frac{2\sqrt{\xi}}{a(1-w)}\right) + \\ & + \mathrm{Li}_2\left(\frac{1+w}{2}\right) - \mathrm{Li}_2\left(\frac{1-w}{2}\right) + \mathrm{Li}_2\left(\frac{a(1+w)}{4}\right) - \mathrm{Li}_2\left(\frac{a(1-w)}{4}\right) \end{aligned} \tag{B4}$$

$$\begin{aligned} t_6 := {} & \ln^2(1+w) + \ln^2(1-w) + \ln\left(\frac{a}{8}\right)\ln(1-w^2) + \\ & + \mathrm{Li}_2\left(\frac{2\sqrt{\xi}}{a(1+w)}\right) + \mathrm{Li}_2\left(\frac{2\sqrt{\xi}}{a(1-w)}\right) - 2\mathrm{Li}_2\left(\frac{2\sqrt{\xi}}{a}\right) + \\ & + \mathrm{Li}_2\left(\frac{1+w}{2}\right) + \mathrm{Li}_2\left(\frac{1-w}{2}\right) - 2\mathrm{Li}_2\left(\frac{1}{2}\right) + \\ & + \mathrm{Li}_2\left(\frac{a(1+w)}{4}\right) + \mathrm{Li}_2\left(\frac{a(1-w)}{4}\right) - 2\mathrm{Li}_2\left(\frac{a}{4}\right) \end{aligned} \tag{B5}$$

$$\begin{aligned} t_7 := {} & 2\ln\left(\frac{1-\xi}{2\xi}\right)\ln\left(\frac{1+v}{1-v}\right) - \mathrm{Li}_2\left(\frac{2v}{(1+v)^2}\right) + \mathrm{Li}_2\left(-\frac{2v}{(1-v)^2}\right) + \\ & - \frac{1}{2}\mathrm{Li}_2\left(-\left(\frac{1+v}{1-v}\right)^2\right) + \frac{1}{2}\mathrm{Li}_2\left(-\left(\frac{1-v}{1+v}\right)^2\right) + \\ & + \mathrm{Li}_2\left(\frac{2w}{1+w}\right) - \mathrm{Li}_2\left(-\frac{2w}{1-w}\right) - 2\mathrm{Li}_2\left(\frac{w}{1+w}\right) + 2\mathrm{Li}_2\left(-\frac{w}{1-w}\right) + \\ & + \mathrm{Li}_2\left(\frac{2aw}{b+aw}\right) - \mathrm{Li}_2\left(-\frac{2aw}{b-aw}\right) - 2\mathrm{Li}_2\left(\frac{aw}{b+aw}\right) + 2\mathrm{Li}_2\left(-\frac{aw}{b-aw}\right) \end{aligned} \tag{B6}$$

$$t_8 := \ln\left(\frac{\xi}{4}\right)\ln\left(\frac{1+v}{1-v}\right) + \mathrm{Li}_2\left(\frac{2v}{1+v}\right) - \mathrm{Li}_2\left(-\frac{2v}{1-v}\right) - \pi^2 \tag{B7}$$

$$\begin{aligned} t_9 := {} & 2\ln\left(\frac{2(1-\xi)}{\sqrt{\xi}}\right)\ln\left(\frac{1+v}{1-v}\right) + 2\left(\mathrm{Li}_2\left(\frac{1+v}{2}\right) - \mathrm{Li}_2\left(\frac{1-v}{2}\right)\right) + \\ & + 3\left(\mathrm{Li}_2\left(-\frac{2v}{1-v}\right) - \mathrm{Li}_2\left(\frac{2v}{1+v}\right)\right) \end{aligned} \tag{B8}$$

$$t_{10} := \ln\left(\frac{4}{\xi}\right), \quad t_{11} := \ln\left(\frac{4(1-\sqrt{\xi})^2}{\xi}\right), \quad t_{12} := \ln\left(\frac{4(1-\xi)}{\xi}\right) \tag{B9}$$

Appendix C

In this Appendix we generalize the cross-section expressions in the main text to include transverse and longitudinal beam polarization effects.¶ The cross section can be written in a matrix factorized form as [26]

$$d\sigma = \left(\frac{2\pi\alpha}{q^2}\right)^2 \sum_{r',r=1}^{4} g_{r'r}(q^2) L^{r'} \cdot H^r dPS, \tag{C1}$$

where $\alpha = 1/137$ is the structure constant, $q^2 = 4E^2_{\rm beam}$ the total quared c.m. beam energy, dPS the Lorentz-invariant phase space element and $L \cdot H$ stands for $L_{\mu\nu}H^{\mu\nu}$. The indices r and r' run over the four independent components of the hadron tensor $H^r_{\mu\nu}$ (defined in Eq. (2)) and the lepton tensor $L^{r'}_{\mu\nu}$, resp. (defined accordingly). $H^r_{\mu\nu}$ stands for the final hadron tensor regardless of whether one is considering polarized or unpolarized final states. In the case treated here (polarized quark), the hadron tensor would carry an additional index labelling the three independent polarization components of the quark. The coefficients of the energy dependent electro-weak coupling matrix $g_{r'r}(q^2)$ are given below. The factorized form of Eq. (C1) has the advantage that the various parts determining the cross section are separated into three modular pieces: $L^{r'}_{\mu\nu}$ contains the angular dependences and the beam polarization parameters, $H^r_{\mu\nu}$ contains the hadron dynamics of the final state and $g_{r'r}(q^2)$ comprises the model dependent parameters of the underlying electro-weak theory.

The electro-weak coupling matrix $g_{r'r}(q^2)$ entering in Eq. (C1) is given by

$$\begin{aligned}
g_{11} &= Q_f^2 - 2Q_f v_e v_f \, Re\,\chi_Z + (v_e^2 + a_e^2)(v_f^2 + a_f^2)|\chi_Z|^2, \\
g_{12} &= Q_f^2 - 2Q_f v_e v_f \, Re\,\chi_Z + (v_e^2 + a_e^2)(v_f^2 - a_f^2)|\chi_Z|^2, \\
g_{13} &= -2Q_f v_e a_f \, Im\,\chi_Z, \\
g_{14} &= 2Q_f v_e a_f \, Re\,\chi_Z - 2(v_e^2 + a_e^2) v_f a_f |\chi_Z|^2,
\end{aligned} \tag{C2}$$

¶Here we return to common usage and call the "alignment" polarization of the electron and positron beam their "longitudinal" polarization.

$$
\begin{aligned}
g_{21} &= q_f^2 - 2Q_f v_e v_f \, Re\,\chi_Z + (v_e^2 - a_e^2)(v_f^2 + a_f^2)|\chi_Z|^2, \\
g_{22} &= q_f^2 - 2Q_f v_e v_f \, Re\,\chi_Z + (v_e^2 - a_e^2)(v_f^2 - a_f^2)|\chi_Z|^2, \\
g_{23} &= -2Q_f v_e a_f \, Im\,\chi_Z, \\
g_{24} &= 2Q_f v_e a_f \, Re\,\chi_Z - 2(v_e^2 - a_e^2) v_f a_f |\chi_Z|^2, \\
\\
g_{31} &= -2Q_f a_e v_f \, Im\,\chi_Z, \\
g_{32} &= -2Q_f a_e v_f \, Im\,\chi_Z, \\
g_{33} &= 2Q_f a_e a_f \, Re\,\chi_Z, \\
g_{34} &= 2Q_f a_e a_f \, Im\,\chi_Z, \\
\\
g_{41} &= 2Q_f a_e v_f \, Re\,\chi_Z - 2v_e a_e (v_f^2 + a_f^2)|\chi_Z|^2, \\
g_{42} &= 2Q_f a_e v_f \, Re\,\chi_Z - 2v_e a_e (v_f^2 - a_f^2)|\chi_Z|^2, \\
g_{43} &= 2Q_f a_e a_f \, Im\,\chi_Z, \\
g_{44} &= -2Q_f a_e a_f \, Re\,\chi_Z + 4v_e a_e v_f a_f |\chi_Z|^2
\end{aligned}
\tag{C2}
$$

where $\chi_Z(q^2) = gM_Z^2 q^2/(q^2 - M_Z^2 + iM_Z\Gamma_Z)^{-1}$, with M_Z and Γ_Z the mass and width of the Z^0 and $g = G_F(8\sqrt{2}\pi\alpha)^{-1} \approx 4.49 \cdot 10^{-5}\mathrm{GeV}^{-2}$. Q_f are the charges of the final state quarks to which the electro-weak currents directly couple; v_e and a_e, v_f and a_f are the electro-weak vector and axial vector coupling constants. For example, in the Weinberg-Salam model, one has $v_e = -1 + 4\sin^2\theta_W$, $a_e = -1$ for leptons, $v_f = 1 - \frac{8}{3}\sin^2\theta_W$, $a_f = 1$ for up-type quarks ($Q_f = \frac{2}{3}$), and $v_f = -1 + \frac{4}{3}\sin^2\theta_W$, $a_f = -1$ for down-type quarks ($Q_f = -\frac{1}{3}$). The left- and right-handed coupling constants are then given by $g_L = v + a$ and $g_R = v - a$, respectively. In the purely electromagnetic case one has $g_{11} = g_{12} = g_{21} = g_{22} = Q_f^2$ and all other $g_{r'r} = 0$. The terms linear in $Re\,\chi_Z$ and $Im\,\chi_Z$ come from $\gamma - Z^0$ interference, whereas the terms proportional to $|\chi_Z|^2$ originate from Z-exchange.

C.1 Lepton tensor

We first specify the lepton tensor in the laboratory frame denoted by a prime. The nonvanishing elements of the lepton tensor $L'^r_{\mu\nu}$ (with $r = 1, 2, 3, 4$ defined in analogy to Eq. (2)) are given by

$$\begin{aligned}
L'^1_{11} &= L'^1_{22} = (1 - h^- h^+), && \text{s} \\
L'^1_{12} &= -L'^1_{21} = -i(h^- - h^+), && \text{a} \\
L'^2_{11} &= L'^2_{22} = -(\xi^-_{x'}\xi^+_{x'} - \xi^-_{y'}\xi^+_{y'}), && \text{s} \\
L'^2_{12} &= L'^2_{21} = -(\xi^-_{x'}\xi^+_{y'} + \xi^-_{y'}\xi^+_{x'}), && \text{s} \\
L'^3_{11} &= -L'^3_{22} = (\xi^-_{x'}\xi^+_{y'} + \xi^-_{y'}\xi^+_{x'}), && \text{s} \\
L'^3_{12} &= L'^3_{21} = -(\xi^-_{x'}\xi^+_{x'} - \xi^-_{y'}\xi^+_{y'}), && \text{s} \\
L'^4_{11} &= L'^4_{22} = (h^- - h^+), && \text{s} \\
L'^4_{12} &= -L'^4_{21} = -i(1 - h^- h^+). && \text{a}
\end{aligned} \tag{C3}$$

Here we have indicated the $\mu \leftrightarrow \nu$ symmetry properties (s=symmetric, a=antisymmetric) of the various components of $L'_{\mu\nu}$ which will be of later convenience when considering the contraction with the hadronic tensor. The $\xi^\pm_{x'}$ and $\xi^\pm_{y'}$ denote the transverse beam polarization in and out of the accelerator plane, and $\xi^\pm_{z'}(= \mp h^\pm)$ the longitudinal polarization (helicity) of $e^\pm$. For natural transverse beam polarization of degree P in the case of a circular accelerator one has $\vec{\xi}^{\pm} = (0, \pm P, 0)$.

C.2 Hadron tensor

In the overall c.m. system that we are considering, only the three space components of the hadron tensors H^r_{mn} $(m, n = 1, 2, 3)$ contribute to the annihilation cross section in Eq. (C1). Also, since the hadron tensors H^r_{mn} are hermitean, there are in general nine real independent components H^r_{mn} for each $r = 1, 2, 3, 4$. We introduce six symmetric and three antisymmetric real combinations under $m \leftrightarrow n$ (dropping the superscript r for compactness) in Table 1, with $H_{\sigma\sigma'} = \varepsilon^\mu(\sigma) H_{\mu\nu} \varepsilon^{*\nu}(\sigma')$, where

$$\varepsilon^\mu(\pm) = \frac{1}{\sqrt{2}}(0; \mp 1, -i, 0), \qquad \varepsilon^\mu(0) = (0; 0, 0, 1). \tag{C4}$$

Table 1 contains the sperical as well as the Cartesian components of the nine independent hadron tensor components in the c.m. system. We also list the $\mu \leftrightarrow \nu$ symmetry properties of the components as well as the parity nature of the product of currents in the helicity system (z-axis in event plane!).

C.3 Angular correlations

We are now in the position to consider the beam-event correlations that arise from the contraction of the lepton and hadron tensors. First we have to rotate the lepton tensors L'_{mn} given in Eq. (C3) to the event plane. This is achieved by the Euler rotation illustrated in Fig. 4,

$$L_{kl}(\varphi,\theta,\chi) = R_{km}(\varphi,\theta,\chi)R_{ln}(\varphi,\theta,\chi)L'_{mn}, \tag{C5}$$

where φ, θ and χ are the Euler angles describing the rotation from the beam-system to the event-system, and the Euler rotation matrix is given by

$$R(\varphi,\theta,\chi) \tag{C6}$$
$$= \begin{pmatrix} \cos\varphi\cos\theta\cos\chi - \sin\varphi\sin\chi & \sin\varphi\cos\theta\cos\chi + \cos\varphi\sin\chi & -\sin\theta\cos\chi \\ -\cos\varphi\cos\theta\sin\chi - \sin\varphi\cos\chi & -\sin\varphi\cos\theta\sin\chi + \cos\varphi\cos\chi & \sin\theta\sin\chi \\ \cos\varphi\sin\theta & \sin\varphi\sin\theta & \cos\theta \end{pmatrix}.$$

Let us note, though, that the contraction $L_{mn}(\varphi,\theta,\chi)H_{mn}$ is simplified by separately considering the symmetric and antisymmetric parts of L_{mn} and H_{mn} according to the classification given in Table 1. Such symmetry considerations are also very helpful when one wants to assess quickly the influence of beam polarization on the measurement of the various hadron tensor components. One obtains (omitting again the superscript r):

$$\begin{aligned} \frac{3}{4}L^1_{mn}H_{mn} &= (1-h^-h^+)H_A + (h^- - h^+)H_D, \\ \frac{3}{4}L^2_{mn}H_{mn} &= X(\varphi)H_B + Y(\varphi)H_C, \\ \frac{3}{4}L^3_{mn}H_{mn} &= X(\varphi)H_C - Y(\varphi)H_B, \\ \frac{3}{4}L^4_{mn}H_{mn} &= (1-h^-h^+)H_D + (h^- - H^+)H_A, \end{aligned} \tag{C7}$$

where

$$
\begin{aligned}
H_A &= \frac{3}{8}(1+\cos^2\theta)H_U + \frac{3}{4}\sin^2\theta H_L + \frac{3}{4}\sin^2\theta\cos 2\chi H_T \\
&\quad -\frac{3}{4}\sin^2\theta\sin 2\chi H_4 - \frac{3}{2\sqrt{2}}\sin 2\theta\cos\chi H_I + \frac{3}{2\sqrt{2}}\sin 2\theta\sin\chi H_5, \\
H_B &= \frac{3}{8}\sin^2\theta H_U - \frac{3}{4}\sin^2\theta H_L + \frac{3}{4}(1+\cos^2\theta)\cos 2\chi H_T \\
&\quad -\frac{3}{4}(1+\cos^2\theta)\sin 2\chi H_4 + \frac{3}{2\sqrt{2}}\sin 2\theta\cos\chi H_I - \frac{3}{2\sqrt{2}}\sin 2\theta\sin\chi H_5, \\
H_C &= \frac{3}{2}\cos\theta\sin 2\chi H_T + \frac{3}{2}\cos\theta\cos 2\chi H_4 \\
&\quad +\frac{3}{\sqrt{2}}\sin\theta\sin\chi H_I + \frac{3}{\sqrt{2}}\sin\theta\cos\chi H_5, \\
H_D &= \frac{3}{4}\cos\theta H_F - \frac{3}{\sqrt{2}}\sin\theta\cos\chi H_A + \frac{3}{\sqrt{2}}\sin\theta\sin\chi H_9,
\end{aligned}
\tag{C8}
$$

with all hadron tensors referring to the event system and

$$
\begin{aligned}
X(\varphi) &= (\xi^-_{x'}\xi^+_{x'} - \xi^-_{y'}\xi^+_{y'})\cos 2\varphi + (\xi^-_{x'}\xi^+_{y'} + \xi^-_{y'}\xi^+_{x'})\sin 2\varphi, \\
Y(\varphi) &= -(\xi^-_{x'}\xi^+_{x'} - \xi^-_{y'}\xi^+_{y'})\sin 2\varphi + (\xi^-_{x'}\xi^+_{y'} + \xi^-_{y'}\xi^+_{x'})\cos 2\varphi.
\end{aligned}
\tag{C9}
$$

Note that H_B and H_C contain no more hadronic structure than H_A. This means that the presence of transverse beam polarization does not increase the number of possible hadronic measurements. On the other hand, transverse beam polarization is helpful in disentangling the hadronic structure.

Eq. (C7) gives the most general structure of possible beam-event correlations in the presence of beam polarization and final state polarization effects. The whole angular dependence on the relative beam-event angles φ, θ and χ is explicitly exhibited in Eqs. (C7) and (C8), since the hadronic helicity structure functions H_α are evaluated in the event frame and thus are independent of these angles. We repeat that, when we have been referring to the hadron tensor in this Appendix, this means either the unpolarized hadron tensor or the polarized hadron tensor carrying any number of additional polarization indices (in our case the quark's polarization index m which can take the three values $m = \perp$ (transversal perpendicular), N (transverse normal) and ℓ (alignment)). Also, in this paper we have only considered the (U)-, (L)- and (F)-components of the hadron tensor in Eq. (C8) which remain after azimuthal φ- and χ-averaging.

References

[1] J.G. Körner, A. Pilaftsis and M.M. Tung, Z. Phys. **C63** (1994) 575

[2] M.M. Tung, Phys. Rev. **D52** (1995) 1353

[3] S. Groote, J.G. Körner and M.M. Tung, "Longitudinal Contribution to the Alignment Polarization of Quarks Produced in e^+e^--Annihilation: An $O(\alpha_s)$-Effect", Mainz preprint MZ-TH/95-09, hep-ph/9507222, to be published in Z. Phys. C

[4] S. Groote and J.G. Körner, "Transverse Polarization of Top Quarks Produced in e^+e^--Annihilation at $O(\alpha_s)$", Mainz preprint MZ-TH/95-17, hep-ph/9508399, to be published in Z. Phys. C.

[5] G. Grunberg, Y.J. Ng and S.H.H. Tye, Phys. Rev. **D21** (1980) 62

[6] J. Schwinger, *Particles, Sources and Fields* (Addison Wesley, New York, 1973), Vol. II, Sec. 5.4

[7] J. Jerzák, E. Laermann and P.M. Zerwas, Phys. Rev. **D25** (1982) 1218; Erratum: **D36** (1987) 310(E)

[8] F. Abe et al. (CDF Collaboration), Phys. Rev. Lett. **75** (1995) 3997

[9] R. Harlander, M. Jeżabek, J.H. Kühn, T. Teubner, Phys. Lett. **B346** (1995) 137;
M. Jeżabek, Karlsruhe preprint TTP 95-12, hep-ph/9503461;
M. Jeżabek, R.Harlander, J.H. Kühn, M. Peter,
Karlsruhe preprint TTP 95-47 (1995), hep-ph/9512409

[10] J.B. Stav and H.A. Olsen, Trondheim preprint (1995); see also
J.B. Stav and H.A. Olsen, Phys. Rev. **D52** (1995) 1359;
J.B. Stav and H.A. Olsen, Z. Phys. **C57** (1993) 519

[11] A.B. Arbuzov, D.Y. Bardin and A. Leike, Mod. Phys. Lett. **A7** (1992) 2029; Erratum: **A9** (1994) 1515

[12] M.B. Voloshin, Int. J. of Mod. Phys. **A10** (1995) 2865

[13] G. Rodrigo and A. Santamaria, Phys. Lett. **B313** (1993) 441;
W. Bernreuther, Aachen preprint PITHA-94/31, hep-ph/9409390

[14] T.D. Lee and M. Nauenberg, Phys. Rev. **B6** (1964) 1594;
A.V. Smilga, Commun. Nucl. Part. Phys. **20** (1991) 69

[15] B. Falk and L.M. Sehgal, Phys. Lett. **B325** (1994) 509

[16] W. Siegel, Phys. Lett. **B84** (1979) 193

[17] J.G. Körner, S. Sakakibara and G. Schuler, Phys. Lett. **B194** (1987) 125

[18] J.G. Körner and M.M. Tung, Z. Phys. **C64** (1994) 255

[19] J.G. Körner, G. Schuler, G. Kramer and B. Lampe, Z. Phys. **C32** (1986) 181;
J.G. Körner, D. Kreimer and K. Schilcher, Z. Phys. **C54** (1992) 503

[20] S. Jadach and Z. Was, Acta Phys. Pol. **B15** (1984) 1151;
Z. Was, Acta Phys. Pol. **B18** (1987) 1099

[21] J.H. Kühn, Acta Physica Austriaca, Suppl. XXIV (1982) 203;
R.H. Dalitz and G.R. Goldstein, Phys. Rev. **D45** (1992) 1531;
F.E. Close, J.G. Körner, R.J.N. Phillips and D.J. Summers,
J. Phys. **G18** (1992) 1716;
T. Mannel and G.A. Schuler, Phys. Lett. **B279** (1992) 194;
B. Mele and G. Altarelli, Phys. Lett. **B299** (1993) 345;
B. Mele, Mod. Phys. Lett. **A9** (1994) 1239;
G. Bonvicini and L. Randall, Phys. Rev. Lett. **73** (1994) 392;
A. Czarnecki, M. Jeżabek, J.G. Körner and J.H. Kühn,
Phys. Rev. Lett. **73** (1994) 384;
A. Czarnecki and M. Jeżabek, Nucl. Phys. **B427** (1994) 3;
J.K. Kim and Y.G. Kim, Phys. Rev. **D52** (1995) 5352;
C. Diaconu, J.G. Körner, D. Pirjol and M. Talby, "Improved Variables for Measuring the Λ_b-Polarization", Mainz preprint MZ-TH/95-28;
C. Diaconu, J.G. Körner, D. Pirjol and M. Talby, "Spin-Momentum Correlations in Inclusive Semileptonic Decays of Polarized Λ_b-Baryons", to be published

[22] M. Anselmino, P. Kroll and B. Pire, Phys. Lett. **B167** (1986) 113;
J.H. Kühn, A. Reiter and P.M. Zerwas, Nucl. Phys. **B272** (1986) 560

[23] W. Bernreuther, J.P. Ma and T. Schröder, Phys. Lett. **B297** (1992) 318;
W. Bernreuther, O. Nachtmann, P. Overmann and T. Schröder,
Nucl. Phys. **B388** (1992) 53; Erratum: **B406** (1993) 516;
A.F. Falk and M.E. Peskin, Phys. Rev. **D49** (1994) 3320;
J.G. Körner and M. Krämer, Phys. Lett. **B275** (1992) 495;
P. Bialas, J.G. Körner, M. Krämer and K. Zalewski, Z. Phys. **C57** (1993) 115

[24] A. Bartl, E. Christova and W. Majerotto,
University of Wien preprint UWThPh-1995-9

[25] C.R. Schmidt, "Top Quark Production and Decay at Next-to-leading Order in e^+e^- Annihilation" (1995) hep-ph/9504434

[26] J.G. Körner and D.H. Schiller, preprint DESY-81-043 (1981)

	spherical components	Cartesian components		
H_U	$H_{++}+H_{--}$	$H_{11}+H_{22}$	s	$pc(pv)$
H_L	H_{00}	H_{33}	s	$pc(pv)$
H_T	$\frac{1}{2}(H_{+-}+H_{-+})$	$\frac{1}{2}(-H_{11}+H_{22})$	s	$pc(pv)$
H_I	$\frac{1}{4}(H_{+0}+H_{0+}-H_{-0}-H_{0-})$	$\frac{-1}{2\sqrt{2}}(H_{31}+H_{13})$	s	$pc(pv)$
H_9	$-\frac{i}{4}(H_{+0}-H_{0+}-H_{-0}+H_{0-})$	$\frac{-i}{2\sqrt{2}}(H_{31}-H_{13})$	a	$pc(pv)$
H_F	$H_{++}-H_{--}$	$-i(H_{12}-H_{21})$	a	$pv(pc)$
H_A	$\frac{1}{4}(H_{+0}+H_{0+}+H_{-0}+H_{0-})$	$\frac{-i}{2\sqrt{2}}(H_{23}-H_{32})$	a	$pv(pc)$
H_4	$-\frac{i}{2}(H_{+-}-H_{-+})$	$-\frac{1}{2}(H_{12}+H_{21})$	s	$pv(pc)$
H_5	$-\frac{i}{4}(H_{+0}-H_{0+}+H_{-0}-H_{0-})$	$\frac{-1}{2\sqrt{2}}(H_{23}+H_{32})$	s	$pv(pc)$

Table 1

Figure Captions

Fig. 1: Born term and $O(\alpha_s)$ contributions to $e^+e^- \to q\bar{q}(g)$. One-loop wave function renormalization graphs are omitted

Fig. 2: y-dependence of the forward-backward component $P_F^\ell(y)$ of the alignment polarization of top quarks produced in the continuum for c.m. energies of 380 GeV (solid), 500 GeV (dashed), 1000 GeV (dashed-dotted) and 1000 TeV (dotted). Also shown is the limiting curve of $P_F^\ell(y)$ for maximal values of y (dotted curve in the upper half of the figure)

Fig. 3: Polar angle dependence of the alignment polarization of
a) top quarks in the continuum for c.m. energies of 380 GeV (solid), 500 GeV (dashed) and 1000 GeV (dashed-dotted)
b) bottom quarks on the Z-peak. Shown are Born term results (dotted) and full $O(\alpha_s)$ results (solid)

Fig. 4: Definition of the Euler angles φ, θ and χ relating the beam frame $\mathcal{O}_{x'y'z'}$ and the event frame $\mathcal{O}_{xyz}$. The three successive Euler rotations from the beam frame to the event frame are $R_{z'}(\varphi)$ followed by $R_{y_1}(\theta)$ and then by $R_z(\chi)$

Caption Table 1

Independent helicity components of the hadron tensor $H_{\mu\nu}$ in the spherical basis (second column) and in the Cartesian basis (third column). Column 4 gives the $\mu \leftrightarrow \nu$ symmetry of the nine components and column 5 lists the parity of the products of contributing currents (pc: VV, AA and pv: VA, AV) for the unpolarized case and in round brackets for the polarized case.

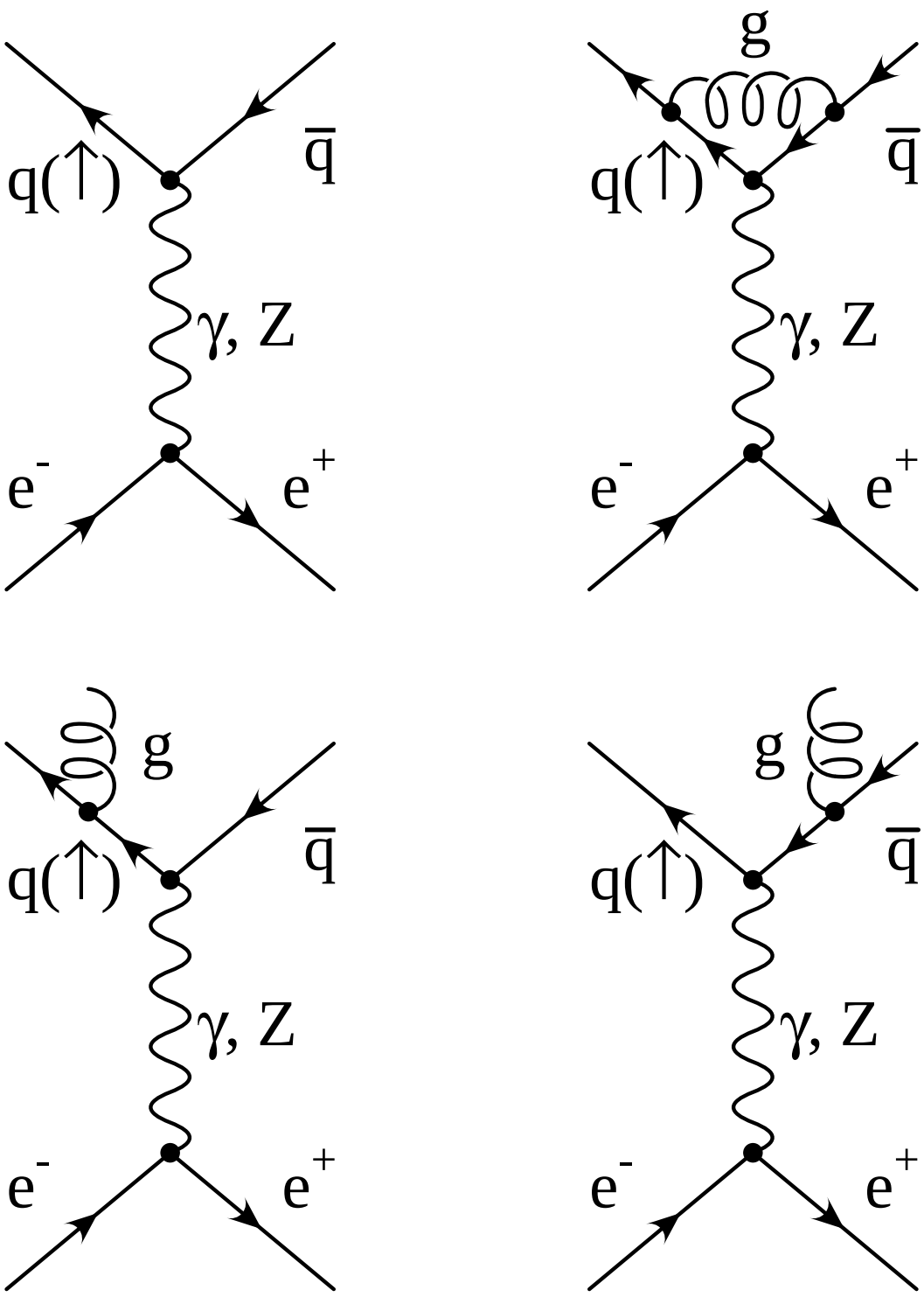

Figure 1

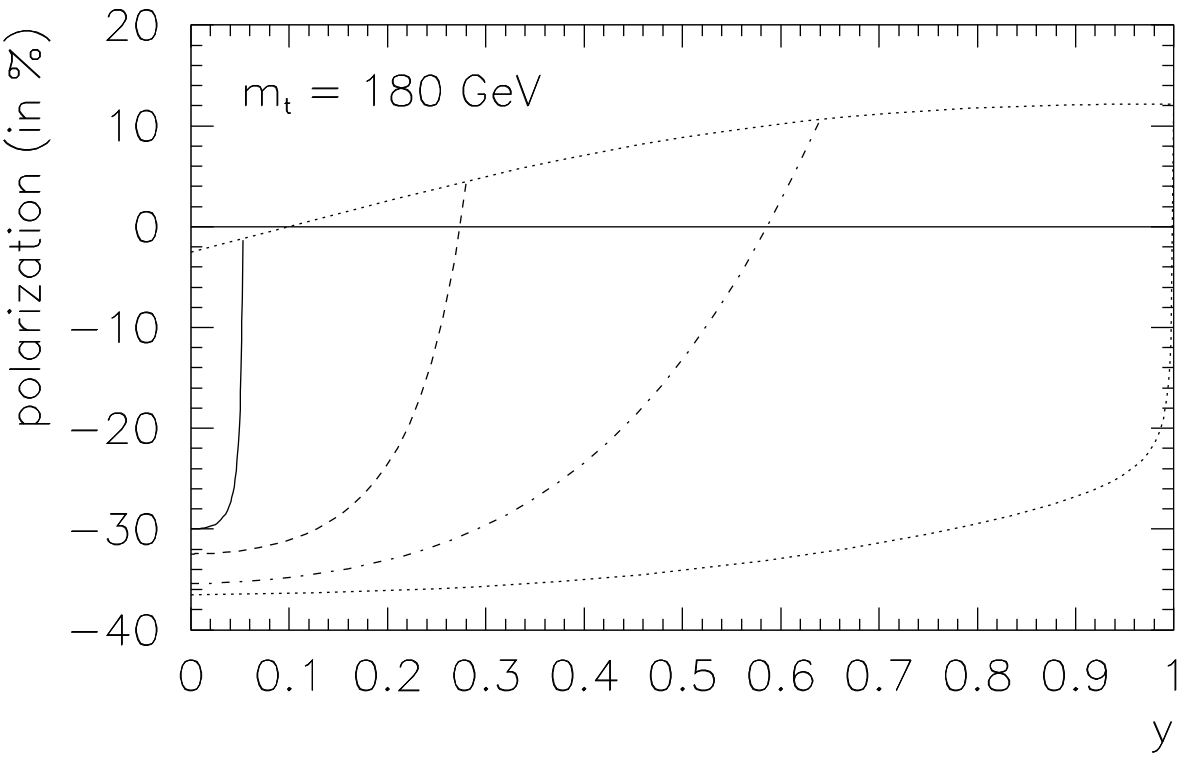
20
10
0
−10
−20
−30
−40
polarization (in %)
m_t = 180 GeV
0
0.1
0.2
0.3
0.4
0.5
0.6
0.7
0.8
0.9
1
y

Figure 2

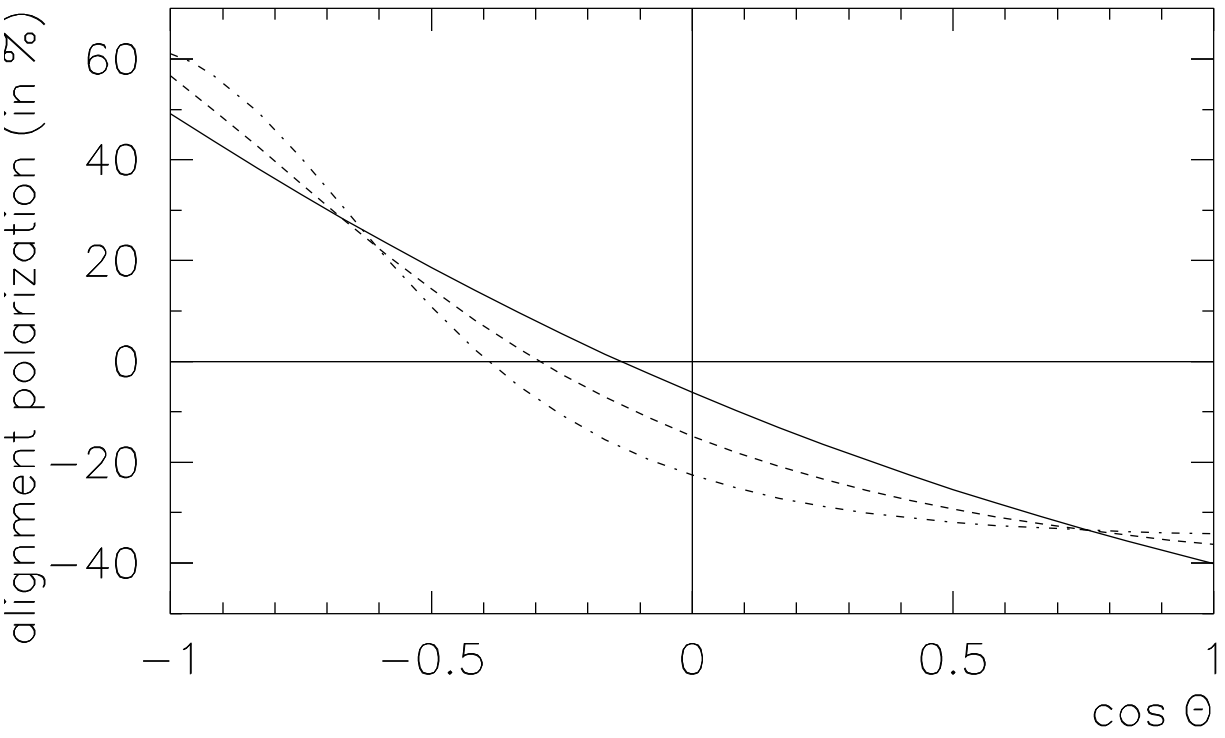

Figure 3(a)

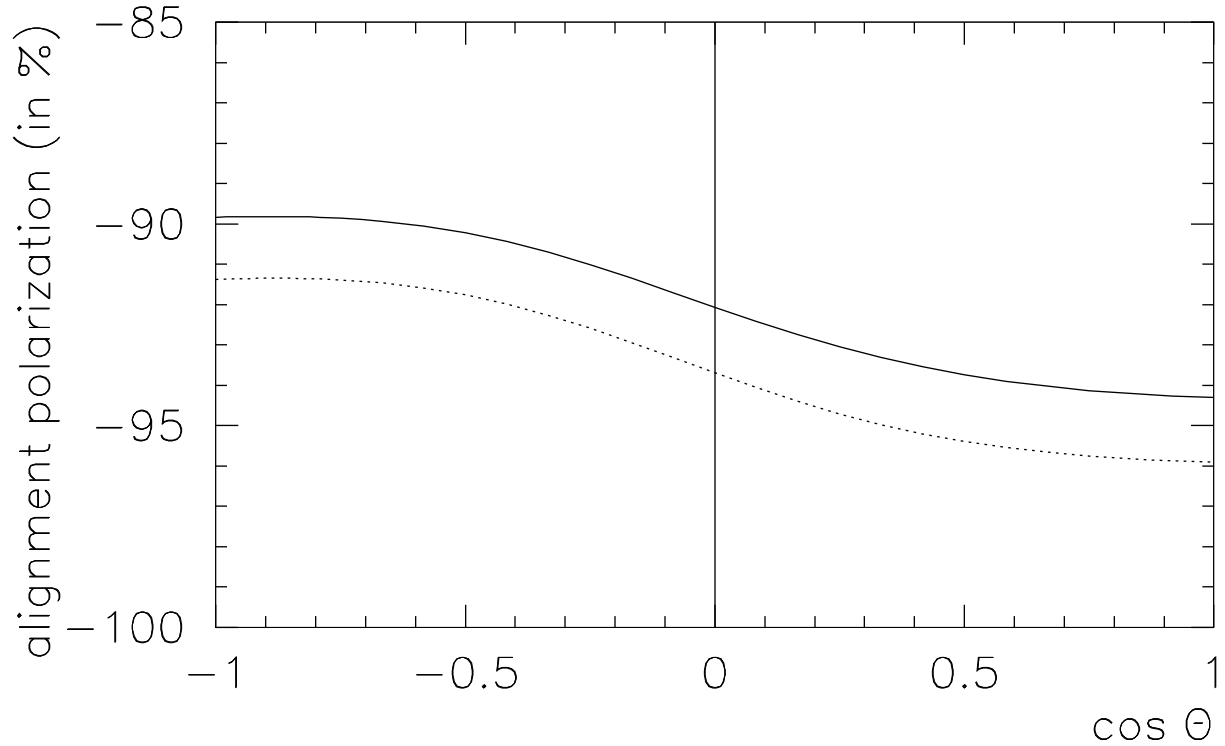

Figure 3(b)

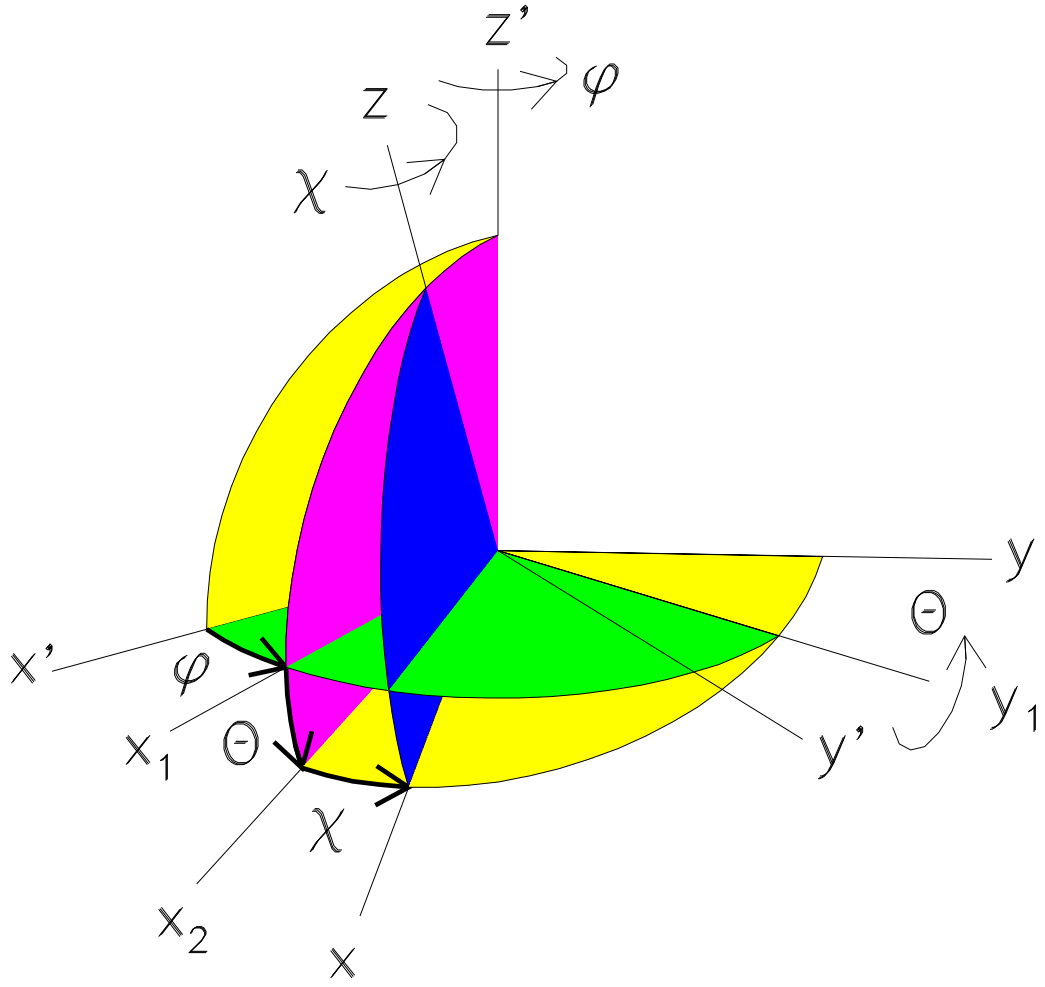

Figure 4